2017-05-01

Developing Hybrid Thickness-Accommodation Techniques for New Origami-Inspired Engineered Systems

Kyler Austin Tolman
Brigham Young University

Developing Hybrid Thickness-Accommodation Techniques for New Origami-Inspired Engineered Systems

Kyler Austin Tolman

A thesis submitted to the faculty of
Brigham Young University
in partial fulfillment of the requirements for the degree of

Master of Science

Larry L. Howell, Chair
Spencer P. Magleby
R. Daniel Maynes

Department of Mechanical Engineering

Brigham Young University

ABSTRACT

Developing Hybrid Thickness-Accommodation Techniques for New
Origami-Inspired Engineered Systems

Kyler Austin Tolman
Department of Mechanical Engineering, BYU
Master of Science

Origami has become a source of inspiration in a number of engineered systems. In most systems, non-paper materials where material thickness is non-negligible is required. In origami-inspired engineered systems where thickness is non-negligible, thickness-accommodation techniques must be utilized to overcome the issue of self-intersection. Many thickness-accommodation techniques have been developed for use in thick-origami-inspired-engineered systems. In this work several thickness-accommodation techniques are reviewed and discussed. New thickness-accommodation techniques including hybrid thickness-accommodation techniques and the split vertex technique are presented and discussed. These techniques enable new capabilities of thickness-accommodation in origami adapted design. Thickness-accommodation techniques have been developed in the context of developable origami patterns and the application of these techniques to non-developable patterns is introduced here. The capability of non-developable thick origami is demonstrated in an application example of a deployable locomotive nose-fairing.

Keywords: Origami, Deployable Mechanisms, Compliant Mechanisms

ACKNOWLEDGMENTS

I would first like to acknowledge and express appreciation for my graduate committee members Dr. Larry Howell, Dr. Spencer Magleby, and Dr. Daniel Maynes for their expertise, inspiration, and guidance throughout the process of my research. I would also like to acknowledge and thank Dr. Robert Lang for his inspiration and collaborative efforts in my research.

I would also like to acknowledge and express thanks to the many members of the Compliant Mechanisms Research Group (CMR) who have helped me with my research and collaborated on the papers that are presented here. Namely I would like to thank Erica Crampton for her collaboration on the thick origami review paper and locomotive fairing project, Chad Stucki and Jeff Niven for their collaboration on the foldable fairing project, Alden Yellowhorse for his collaboration on the non-developable origami work, and Michael Morgan for his work on the offset-panel technique which led into my work on hybrid-thickness-accommodation techniques. I would also like to thank the other members of the CMR who I have had the privilege of working together with on various projects and publications that are not included in this thesis.

Finally I would like to thank my family for their continued support and encouragement throughout my schooling. I would like to express appreciation for my wife Ann for her love, support, and patience with me on this journey. Her determination to help me become a better person is what persuaded me to pursue graduate school.

This work is based upon research supported by funding from the National Science Foundation and the Air Force Office of Scientific Research under Grant No. 1240417. Any opinions, findings, and conclusions or recommendations expressed in this thesis are those of the authors and do not necessarily reflect the views of the National Science Foundation.

TABLE OF CONTENTS

LIST OF TABLES

LIST OF FIGURES

CHAPTER 1. INTRODUCTION

The ancient art of origami has become a source of inspiration for scientists and engineers. Origami has inspired the design of devices as small as medical stents [1] and as large as space solar arrays [2]. The shape-changing ability of origami has made it attractive for many engineering problems where space is a constraint or unique motion is desirable.

Origamists traditionally create objects by folding thin paper. Most engineering applications however require devices that are made of strong and stiff materials. Many origami patterns can be folded because paper is thin and can fold flat upon itself. If these same origami patterns folded in paper were transferred to a thick material by adding hinges where the creases were located, the pattern would not fold flat due to panel interference. Enabling origami patterns to fold in a material with thickness is a critical step in creating an origami-based solution to engineering problems.

Origami can be seen as a series of hinges and panels [3]. Many techniques have been developed for accommodating thickness in origami design. These techniques involve either modifying the origami pattern's folding axes (hinges), panels, or the pattern itself. Each technique offers its own set of capabilities and limitations. The thickness-accommodation technique that best suits a particular design problem largely depends on the constraints of the problem and the origami pattern involved. In chapter two, a review of the major existing thickness-accommodation techniques is given. This chapter is taken from a review paper on thickness-accommodation in origami-adapted design that has been accepted for publication [4].

Much effort has gone into the development of several different thickness-accommodation techniques, however, until recently, efforts had not been made to combine the various techniques. In chapter three, hybrid techniques, which combine two or more thickness accommodation techniques are introduced here for the first time. Hybrid techniques offer an interesting alternative for designers who wish to incorporate the strengths of multiple techniques into one application. This chapter on hybrid techniques also comes from the recently accepted review paper [4].

Although several different thickness-accommodation techniques have been developed, there still exists much opportunity to create additional techniques. One of the drawbacks of many thickness-accommodation techniques is that they create holes in pattern at the vertices. While small holes at the vertices may be acceptable in some applications, this becomes a challenge in applications where a sealed surface must be maintained. To address the issue of verticial holes in thick origami chapter four introduces a new thickness-accommodation technique called the split-vertex technique. This technique involves modifying a crease pattern so that thick panels will have space within the pattern to stack. The mechanisms that result from the split-vertex technique are single-degree-of-freedom mechanisms composed of spherical linkages that do not have any holes at the vertices. This new technique incorporates some of the methods of existing techniques and can be classified as a hybrid technique with its own unique design considerations and capabilities. Several application examples of this technique are also shown. This chapter is taken from a conference paper that has been accepted for publication [5].

Chapter five introduces the application of thickness-accommodation techniques to non-developable origami patterns. Because origami is traditionally folded from a flat piece of material, the majority of patterns used in thick origami have been patterns that fold out flat. These patterns are called developable as they can be flattened without any stretching of the panels in the origami pattern. Because many engineering applications require shapes that are not flat, folding non-developable shapes that are constructed from thick materials is an area of particular interest.

Chapter six applies these principals of thick origami to the development of a non-developable thick-origami-based deployable locomotive nose fairing. The use of origami in an aerodynamic application is a unique challenge because the folding principles of origami must be balanced with aerodynamic considerations. This fairing must meet a highly constrained design space and the shape is optimized using CFD analysis and optimization techniques. Origami is applied to the resulting optimized shape to create a fairing which can easily stow and deploy within the design constraints. Prototypes of the fairing are constructed and shown to validate its operational feasibility. This fairing is estimated to reduce overall aerodynamic drag on the locomotive by 16% at a 80 kph velocity.

The objective of this research is to enable new capabilities of thickness-accommodation in origami-adapted design by developing new techniques. This will allow designers to create origami-

inspired engineered systems that overcome many of the challenges of existing approached and have unprecedented performance. This objective is met by developing hybrid techniques which combine existing methods, introducing the split-vertex thickness accommodation technique which solves the issue of holes at vertices, applying thickness-accommodation techniques to non-developable patterns, and showcasing these techniques in the development of a non-developable thick-origami based deployable locomotive fairing.

CHAPTER 2. A REVIEW OF THICKNESS-ACCOMMODATION TECHNIQUES

In this chapter, a review of the many techniques that have been developed to address the challenges of folding mechanisms where the thickness of the facet materials is non-negligible in the mechanism design will be presented. This review is part of a recently accepted review paper about thickness-accommodation in origami-inspired engineering [4]. While thick folding mechanisms have been demonstrated and used for decades, the first two decades of the current millennium have been especially productive for their study; several research groups have developed distinct techniques for handling thickness. This review summarizes the various approaches, including those that have been developed at this University, and discusses their strengths and limitations.

2.1 Tapered Panels Technique

The tapered panels technique for accommodating thickness in origami was an early technique that fully preserved the kinematics of the zero-thickness model [6]. The underlying principle governing this technique is that the same zero-thickness surface from the original origami model still exists within the mechanism and thickness is added around that surface. Hence, another descriptive name for this technique is "embedded zero-thickness surface" [7]. Figure 2.1 shows the technique applied to a Miura-ori pattern.

How the tapered panels technique is generally applied is illustrated in Figure 2.2. As shown by the "thickness added" step, material is added equally to each side of the zero-thickness surface to thicken the panels to the required total thickness. To determine the taper necessary for each panel in the mechanism to avoid intersection with its neighbors, a thickened model can be folded and the volume of the panels trimmed along the bisection of the dihedral angle at each joint. To maintain a non-zero panel thickness, the maximum fold angle of the thick origami mechanism cannot reach 180°.

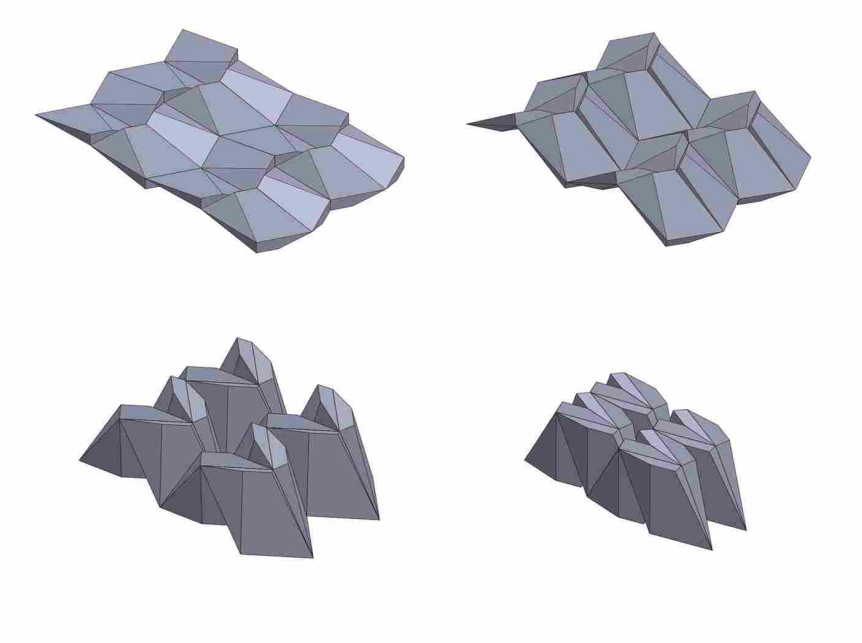

Figure 2.1: Tapered panels technique applied to the Miura-ori pattern.

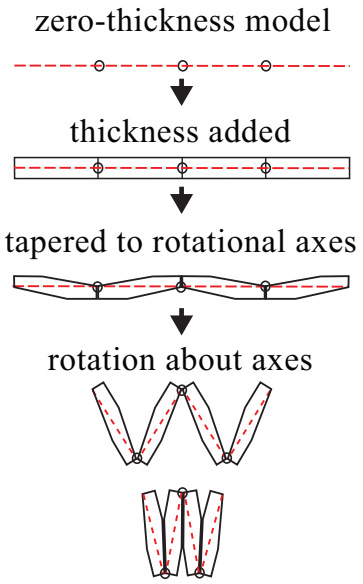

Figure 2.2: The tapered panels technique.

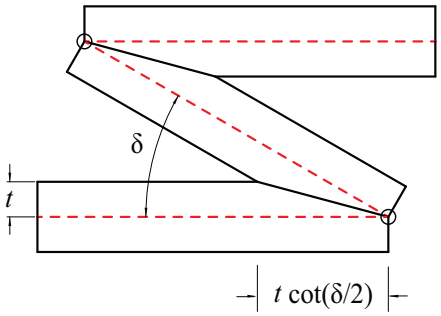

Figure 2.3: Diagram detailing the length of a panel's taper.

The length of the taper on the zero-thickness panel, as found in [6] and detailed in Figure 2.3, is given by

$$t\cot(\delta/2) \tag{2.1}$$

where t is the half thickness of the panel (i.e. the maximum distance from the zero-thickness surface to the outer face of the panel), and δ is the dihedral angle of the embedded zero-thickness facets at the maximum folded state.

There are a few notable characteristics of the tapered panels technique. By adding material to the outside of the vertices in a similarly tapered fashion, it is possible to limit the unfolded state so that the zero-thickness pattern cannot reach its "flat" unfolded position, thereby achieving a potentially desirable non-flat state and avoiding singularities in the motion space that could allow undesirable movements. Also, as the technique cannot accommodate fold angles of 180° (in the zero-thickness reference), singularities in the flat-folded state can be similarly avoided. However, this property also carries with it two potential inefficiencies. First, in a single-DOF mechanism, the relative spacing of all panel pairs is defined by a single quantity; at the maximally folded state, some panels may be closely spaced, while others may be separated by larger amounts. It is generally not possible to individually tune panel spacings for maximum packing. Second, the packing efficiency of the mechanism generally decreases as the thickness of the panels is increased because the motion must halt farther away from the flat-folded state. [6]

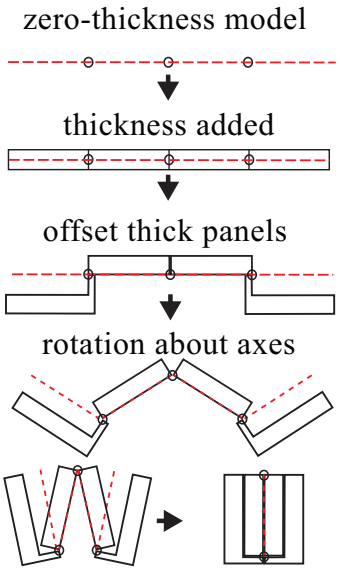

Figure 2.4: The offset panel technique.

2.2 Offset Panel Technique

Edmondson et al. proposed a thickness-accommodation technique that also maintains the same kinematics as the zero-thickness model, but rather than trimming material away from panels to avoid interference, offsets are used to position the panels away from the zero-thickness surface [8, 9]. This method, as illustrated in Figure 2.4, allows for a fully collapsed position where panels lie parallel to and in contact with each other, and achieves the full range of angular motion of the zero-thickness equivalent surface. The underlying principle behind the offset panel technique is that all the rotational axes lie within the same plane as the zero-thickness model in both the unfolded and flat-folded states, creating a mechanism that is kinematically equivalent to the original origami pattern. This allows the panels themselves to be displaced individually as needed to avoid self-intersection.

This technique is implemented via a series of steps: thickening the origami pattern's panels, stacking the panels in the fully folded position, selecting a zero-thickness reference plane, creating offsets that join the stacked panels to the rotational axis locations of the zero-thickness origami model, and modifying panels to avoid self-intersection [9].

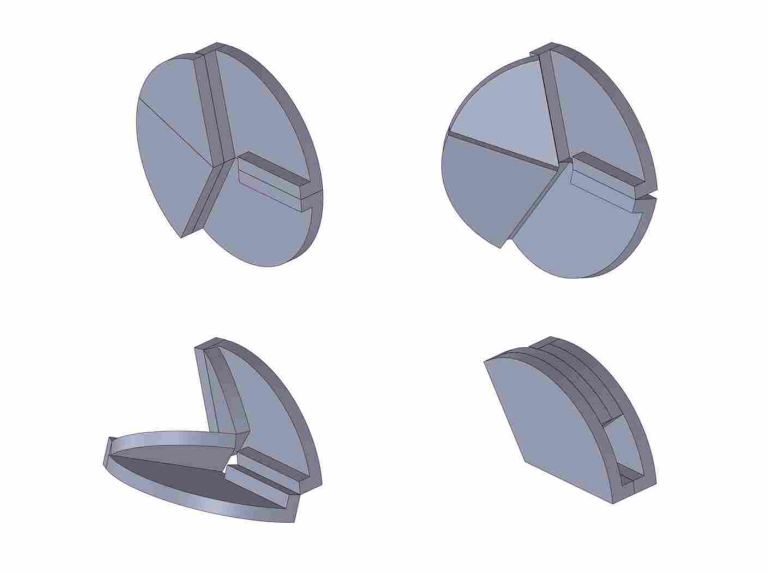

Figure 2.5: A single offset panel vertex.

A characteristic of the offset panel technique is that, in the unfolded state, the pattern is no longer planar but contains multiple elevations, as illustrated in Figure 2.5. The offset panel technique offers flexibility to the designer in the choice of where to place the zero thickness plane, how to construct the offsets, and allows the thickness of each panel to vary with respect to that of the other panels.

However, the offset panel technique brings with it its own challenges. Those include the stresses that occur at hinges due to long offset lengths, as well as accommodating the additional geometry of the offsets themselves. Because all panels connect to the zero-thickness reference model, cut-outs are also often required in some panels to allow the offsets of other panels to access the zero-thickness reference plane.

Despite the challenges that arise in the offset panel technique, the ability to work with any arbitrary origami pattern and the flexibility offered to use panels of varying thickness make it a viable method for the design of products. Morgan et al. demonstrated the offset panel technique in the development of several potential product applications including a kinetic sculpture, foldable circuit board, electrical engineers toolbox, and foldable table [10]. The same work also demonstrated how the geometry of the panels can be varied not only in thickness, but also in any other dimension, as long as the rotational axes remain in their relative positions and panels do not intersect.

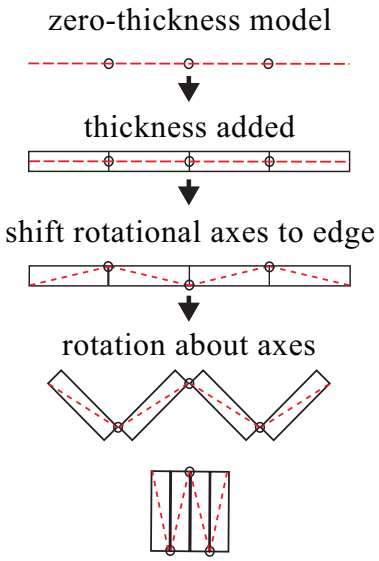

Figure 2.6: The hinge shift technique.

2.3 Hinge Shift Technique

The hinge shift technique as illustrated in Figure 2.6 accommodates thickness and avoids interference by shifting the location of the rotational axes away from a single plane. While moving rotational joints to the faces of thick panels can be seen even in 19th-century patent literature [11–13], complexity with such an approach arises when dealing with interior vertices.

The simplest form of accommodating thickness, though only applicable to single line folds, is to move the joint axis to the valley side of the fold, what Tachi called "axis-shift" [6]. The method of shifting hinges at a thickened interior vertex to allow for folding was demonstrated by Hoberman [14] for a symmetric bird's foot vertex used in the Miura-ori pattern [15]. This thick folding vertex, as shown in Figure 2.7, utilizes two levels of thickness (where the thicker portion is simply twice the thickness of the other), with rotational axes placed on each of the faces to achieve a one-DOF motion from a completely flat to completely folded state.

A limitation of this implementation of the hinge shift technique is that only the symmetric bird's foot vertex can be thus accommodated. Despite this limitation, there are many useful origami patterns that make use of the symmetric bird's foot vertex. We show an example in Figure 2.8

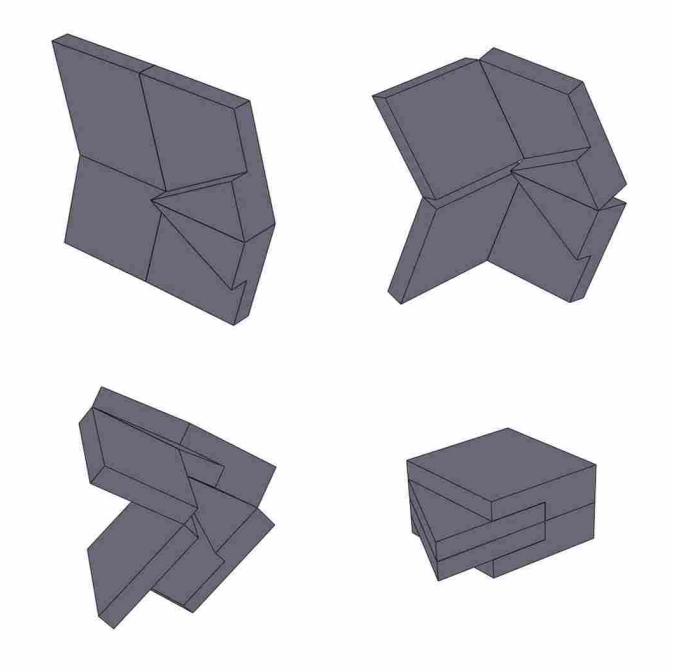

Figure 2.7: A thick folding vertex demonstrated by Hoberman for the Miura-ori pattern.

of this approach applied to the Yoshimura pattern [16], also known as the arc pattern [17], or accordion pattern [18].

Furthermore, by introducing different shifts, other types of vertices can, in fact, be accommodated, as we will presently show.

Trautz et al. demonstrated another implementation of shifting hinges, illustrated in Figure 2.9. This approach shifts the hinge axes by incorporating translation into the hinges themselves [19]. In this approach, the offset distances are constrained to the thickness of the panels and the mechanism is allowed to fold through the use of sliding hinges. The sliding hinges give the mechanism the added degrees of freedom to function, but consequently result in a vertex with several additional degrees of freedom. In addition, the accumulated sliding can result in mechanical interferences, therefore requiring a reduced range of motion [20].

De Temmerman et al. [21, 22] demonstrated an implementation similar to Hoberman's for a degree-6 thickened vertex used in the Yoshimura pattern [16] as shown in Figure 2.10. This type of joint utilizes a single thickness layer with all fold axes placed on either the top or bottom face of the panels. While such a joint can be used to create a thick panel folding Yoshimura pattern as shown in Figure 2.11, De Temmerman alternatively utilized the joint in a folding bar structure.

Figure 2.8: Photos of a thickened rigidly-foldable arc pattern prototype created using symmetric degree-4 vertices shown moving from flat to folded.

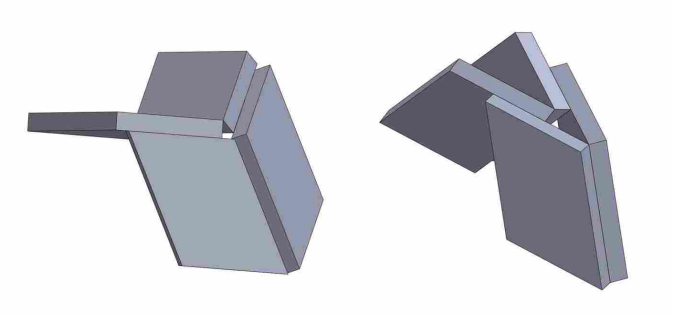

Figure 2.9: The sliding hinge approach demonstrated by Trautz et al.

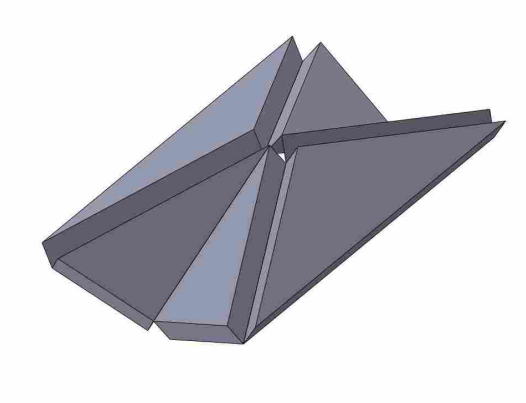

Figure 2.10: A thick folding vertex demonstrated by De Temmerman for the Yoshimura pattern.

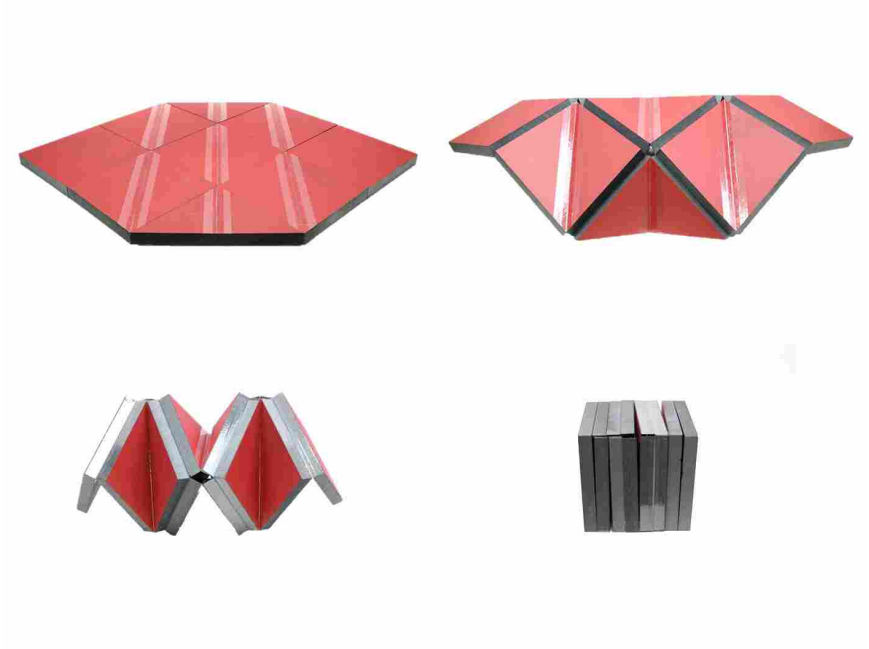

Figure 2.11: Photos of a thick folding Yoshimura pattern prototype comprised of symmetric degree 6 vertices.

More recently, Chen et al. showed an implementation that generalizes hinge shifting to encompass the symmetric bird's foot and Yoshimura-pattern axis-shifted vertices and also includes non-symmetric thick vertices [23]. Their work made the connection between well-studied 4, 5, and 6R spatial linkages and the hinge-shifted vertices of a thick panel origami pattern.

For a 4R spatial linkage, the only known linkage is the Bennett linkage [24]. While the vertex demonstrated by Hoberman is a Bennett linkage, it is only a particular case of the Bennett linkage. Connecting this thick folding vertex to the Bennett linkage has enabled a greater range of vertex geometries to be accommodated using the hinge shift technique. One example of how this work has expanded the applicability of the hinge shift technique is shown in Figure 2.12 as it is applied to a rigidly foldable square twist pattern.

The general case of a spatial 4R linkage being applied to a thick degree-four vertex is shown in Figure 2.13. In this model, four sector angles (α_1,α_2,α_3, and α_4) and four offset distances (d_1, d_2, d_3, and d_4) describe the geometry of the linkage. For the 4R spatial Bennett linkage, opposing link pairs are equal in length and have the same rotational axis twist [25]. The criteria for the

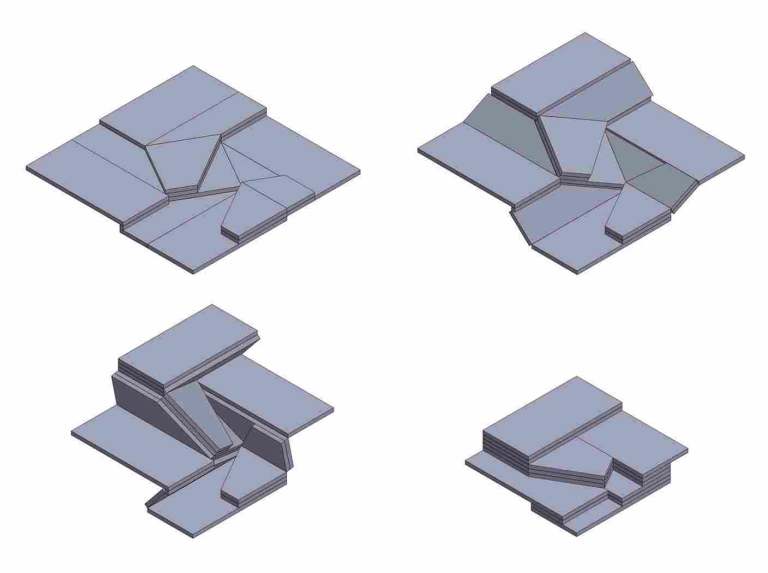

Figure 2.12: A thick rigidly foldable square twist developed using the generalized hinge shift technique of Chen et al.

mechanism to achieve mobility given in [23, 26] are:

$$\alpha_1 + \alpha_3 = \alpha_2 + \alpha_4 = \pi \tag{2.2}$$

$$d_1 = d_3, d_2 = d_4 \tag{2.3}$$

$$\frac{d_1}{d_2} = \frac{\sin(\alpha_1)}{\sin(\alpha_2)} \tag{2.4}$$

It is interesting to note that the criteria listed in Equation (2.2) corresponds with the flat foldability criteria which is:

$$\alpha_1 - \alpha_2 + \alpha_3 - \alpha_4 + \ldots = 0. \tag{2.5}$$

This establishes that, for a degree-4 vertex, the hinge shift technique can only be applied to flat foldable patterns.

Chen et al. have also expanded this technique to encompass some higher-order vertices. The 5R Myard linkage [27] gives rise to hinge-shifted degree-5 vertices and the 6R Bricard linkage [28] was utilized for degree-6 vertices [29]. The 5R and 6R linkages implemented in these vertices are single-DOF mechanisms and consequently the thick origami mechanisms are also single-DOF.

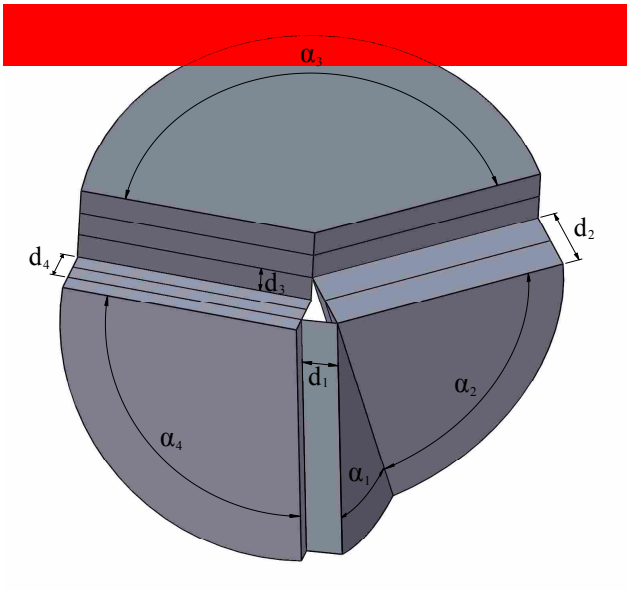

Figure 2.13: A generalized thick folding vertex demonstrated by Chen et al.

2.4 Doubled Hinge Technique

The general principle of the doubled hinge technique is to split fold lines into two fold lines thereby expanding the crease area to allow for the thickness of the panels. A method of splitting fold lines for the purpose of accommodating stacked layers was demonstrated by Hoberman [30] in the modification of a map fold pattern. While Hoberman's method aims to allow panels to fold efficiently, it must be noted that it is a crease modification technique, not a thickness-accommodation technique and would still require a subsequent step utilizing one of the thickness-accommodation techniques discussed in this review paper. Zirbel et al. showed how Hoberman's concept of splitting a vertex in conjunction with the membrane technique can be used in the design of solar array packing [31]. The membrane technique (discussed in Sec. 2.6) approaches thickness accommodation similarly by widening a crease with flexible material.

Ku and Demaine introduced the offset crease technique for thickness accommodation [32], which is an implementation of the doubled hinge technique where every crease is split in two. They further provided detailed analysis of the desired splitting widths for arbitrary patterns. This technique, as shown in Figure 2.14, modifies the zero-thickness model by splitting each fold line into two fold lines. The modified zero-thickness model then remains in the middle of the thick panels and material is trimmed away from the panels to prevent self intersection similar to the

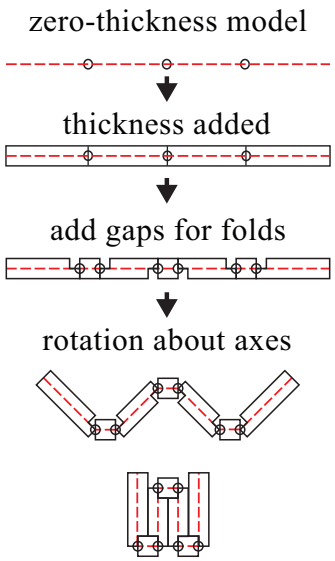

Figure 2.14: The doubled hinge technique (offset crease implementation).

tapered panels technique. An advantage that the offset crease technique has over the tapered panels technique is that each fold line only undergoes folding of 90° rather than 180° and consequently less material needs to be trimmed to prevent self intersection. Mechanisms using this technique also maintain the ability to move from a fully flat state to a fully flat-folded state.

A requirement of this technique is that cutouts be present at the vertices of the pattern in both the flat and folded states to prevent self-intersection during folding. A cutout disconnects the folds at the vertex and, in concert with the doubling of the number of folds around the vertex, adds additional degrees of freedom to the mechanism.

A simple degree-4 vertex, such as the one shown in Figure 2.15, using the offset crease technique typically has a loop of eight creases, thus two degrees of freedom. One degree of freedom in the offset crease vertex is the amount by which the mechanism is folded; the other degree of freedom is an orthogonal independent degree of freedom that allows "wiggliness" or play in the vertex for a given intermediate fold state. It has been shown that a kinematic path exists between the flat and fully-folded states generated by this technique [33].

In Sections 2.5 and 3.2, an implementation of the doubled hinge technique where select creases are doubled for use in conjunction with the rolling contact technique [7] is shown. While it is possible that an entire approach can be formed on the concept of selectively doubling hinges, this is left open for future work.

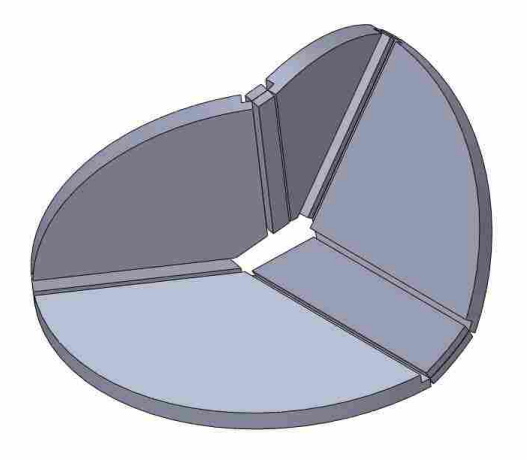

Figure 2.15: An offset crease implementation of the doubled hinge technique demonstrated for a single degree-4 vertex.

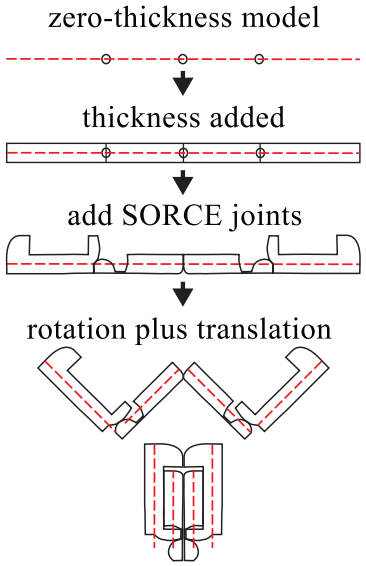

Figure 2.16: The rolling contacts technique (SORCE implementation).

2.5 Rolling Contacts Technique

Like many concepts relevant to thick origami, rolling contacts have 19th-century roots; a familiar example of a rolling contact joint is the Jacob's ladder toy over a hundred years old [34,35]. Recent advances, however, have made it possible for this type of joint to be used in engineering applications such as prosthetic knee joints [36], spinal implants [37], and robot fingers [38]. A sig-

nificant refinement came with compliant contact-aided mechanisms that utilize compliant flexures to maintain contact and to enforce a non-slip condition between the rolling faces [39, 40]. Such joints can be used in thick-folding mechanisms; in fact, Cai gave a kinematic analysis of cylindrical rolling joints that allow for folding of thick plate structures as an alternative method for thickness accommodation in planar mechanisms [41].

In a further generalization of rolling contacts, Lang et al. presented a generalized technique that utilizes Synchronized-Offset Rolling-Contact Elements (SORCE) to achieve kinematic single-DOF motion in thick origami-inspired mechanisms [7]. This technique, illustrated in Figure 2.16, utilizes rolling contacts with profiles that have been synthesized to achieve the same dihedral angles as a zero-thickness origami model while creating dynamically varying transverse offsets that address non-self-intersection. Prior to this work, rolling contacts had only been utilized for planar mechanisms and had not dealt with thickness accommodation at interior vertices of an origami pattern. A notable aspect of the SORCE technique is that it marries a fully flat unfolded state (where all primary panel areas are coplanar, not necessarily including the joints) with a folded state incorporating arbitrary offsets between panels; furthermore, the DOF of the mechanism exactly reproduces the DOF of the zero-thickness model. Single-DOF mechanisms such as the Miura-ori or split square twist will remain single-DOF when implemented as SORCE joints. In fact, the technique can be applied to any arbitrary origami pattern containing any combination of vertices of varying degree.

The SORCE technique overcomes some of the difficulties that arise in other techniques because it is able to accommodate panels of arbitrary thickness, maintain the full range of motion, and preserves kinematic single-DOF motion (if it was present in the zero-thickness reference). The SORCE technique uses a unique way of achieving a translating zero-thickness plane for each panel. All of the zero-thickness planes begin coplanar in the unfolded state and then each panel offsets along an individual and specified path throughout the motion of the mechanism. The rate of offset of the individual panels relative to the zero thickness model is synchronized between the panels by the shapes of the rolling contacts to be pairwise consistent at each fold, hence the name "synchronized offset".

However, like all of the techniques, SORCE joints have their own special considerations. The rolling contact surfaces are uniquely specified by the desired motion and offsets, but the cur-

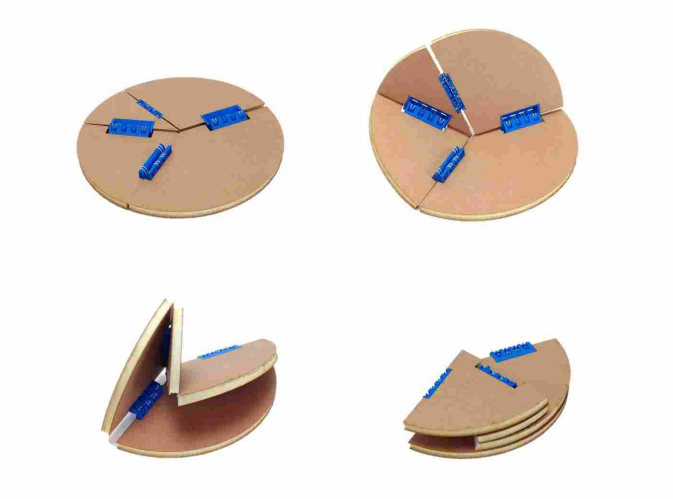

Figure 2.17: A prototype of thick vertex utilizing SORCE technique demonstrated by Lang et al.

vature and convexity of the rolling contact surfaces must be taken into account during design to ensure robust joints.

In [7], the authors gave analytic prescriptions for computing the shapes of rolling contacts for vertices in which the panel offsets were purely perpendicular to the panels (which apply to any degree-4 vertex) and those that combine perpendicular and lateral offsets (which only apply to certain special cases). Several examples were given along with proof-of-concept prototypes such as the one shown in Figure 2.17.

There is an interesting duality between the SORCE technique and the hinge shift technique of Trautz et al. [19]. In that latter, the panels are allowed to shift *along* the axes of the hinges throughout the range of motion. In the former, the panels are allowed to shift *in the two perpendicular directions* relative to the axes, and, in fact, that type of rolling contact cannot accommodate *any* shift along the axes.

2.6 Membrane Technique

Though thin membranes have been used before for prototyping thick origami, using the membrane itself to accommodate panel thickness was fully explored by Zirbel et al. [2]. Thin membranes, such as fabric, were previously used primarily to simulate ideal hinges that have the

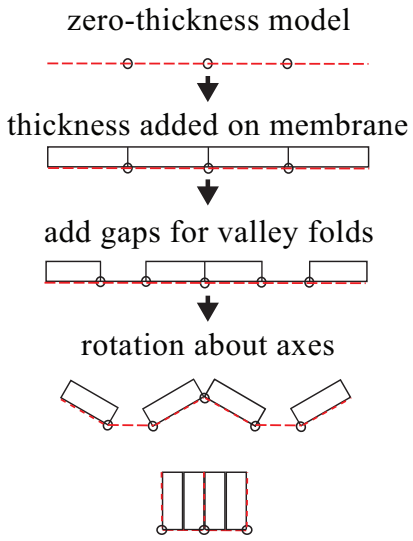

Figure 2.18: The membrane technique.

center of rotation exactly at the seam between panels. However, a thin membrane can be used to accommodate thickness in origami as illustrated in Figure 2.18.

When using this technique, the panels of the mechanism are connected by a thin membrane that can, in contrast to the panels themselves, be treated as approximately zero-thickness. By increasing the spacing between panels for valley folds, the membrane can not only serve as the hinge, but also accommodate the thickness of the panels to allow folding. For a rigidly foldable origami pattern, the maximum spacing between panels necessary for a 180° valley fold is $2t$ where t is the thickness of the panels. When the final desired valley fold angle is less than 180°, the spacing can be decreased accordingly; for example, fold angles of 90° and 60° would require spacings of $\sqrt{2}t$ and t, respectively.

While conceptually simple to implement, modeling flexible membrane hinges is considerably more complicated than mechanisms with discrete hinges. Recent work by Peraza-Hernandez et al. laid out a computational model for such mechanisms [42]. Further complicating the modeling is the observation that the state space for motion is extremely high-dimensional, and the path through state space of a folded state as it deploys is typically determined by energy minimization

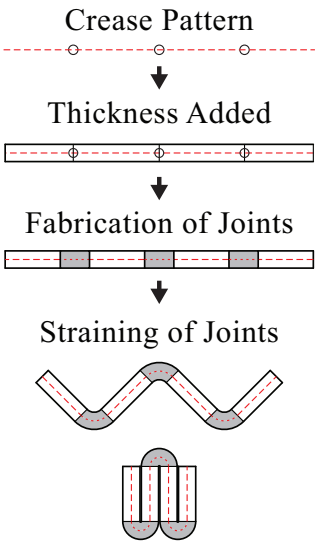

Figure 2.19: The strained joint technique.

along the path; thus, one must model strain energy within the curved hinges in order to determine actual motion and reachability.

Mechanisms using the membrane thickness-accommodation technique have extra degrees of freedom when compared to their ideal zero-thickness origami models. In this way, the technique is closely related to the offset-crease technique (Sec. 2.4) as it widens the crease area to allow for the panels to meet and does not guarantee consistent motion. As this crease widening increases the number of hinge points, it results in the mechanism having extra degrees of freedom. However, these extra degrees of freedom can be advantageous in allowing folding of a pattern that is otherwise not entirely rigid-foldable [2, 31]. Also, because of the flexibility of the membrane, it may be necessary to keep tension at the edges of the mechanism in the unfolded configuration.

2.7 Strained Joint Technique

The strained joint technique for accommodating thickness, introduced by Pehrson et al. [43], is related to the membrane technique. Instead of using a thin membrane, the thick material itself acts as an effective membrane, i.e., one in which the "fold" is distributed across a region, rather than being a discrete revolute joint. In this case, the panel material itself is dissected so as to be flexible along desired hinge lines as seen in the illustration of the strained joint technique shown in Figure 2.19. This gives an entirely monolithic mechanism, as can be seen in Figure 2.20.

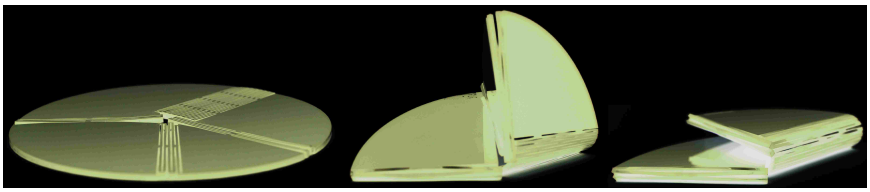

Figure 2.20: The strained joint technique applied to a degree 4 vertex.

To create flexible joint areas in the otherwise rigid panel material, surrogate folds are introduced in the design. A surrogate fold is "a localized reduction in stiffness achieved through geometry to allow non-paper materials to achieve similar behaviors to a fold in paper" [44]. An important characteristic of these surrogate folds is that the folding motion does not cause the material to plastically yield; all deformations remain within the elastic regime despite large-angle flexing. Although putting strategic cuts in materials to reduce stiffness has been used previously to improve the accuracy and decrease the effort required in sheet metal bending where yielding is desired [45], it has not been widely used for the purpose of repeated motion, i.e., motion remaining within the elastic regime.

Surrogate folds are compliant joints [46]; examples of some geometries that can be used as surrogate folds can be found in [47]. Delimont et al. have evaluated several other potential geometries for use as surrogate folds in origami-inspired mechanisms that are suited to either resist or be predisposed to particular motions and deflections [44, 48].

By arraying these surrogate fold geometries in series and parallel, the amount of deflection can be customized and tailored to meet the fold characteristics required at each crease of the origami pattern. The strain allowed in the surrogate folds without material yielding is what enables the motion of the origami, hence, the term "strained joint technique." It should be noted that the membrane technique also involves strain, localized within the membrane hinges. In this case, however, the strain takes place within the same material that constitutes the panels.

Pehrson et al. have outlined the primary design approach for applying the strained joint technique to a fold pattern [43]. Material and origami crease pattern selection occur first. Material selection holds particular importance in this technique for thickness accommodation because the motion of the joints in the mechanism results from material deflection, which is, in turn, governed by material properties. When using arrays of lamina-emergent torsion (LET) joints for the

surrogate folds, a material with a high ratio of yield strength to shear modulus of elasticity is desired [49].

After material and crease pattern selection, the creases are tagged according to how many layers of material must be accommodated by the joint at that crease; only then can the joints themselves be fully designed. Because the motion of the mechanism is a result of material deflection, fatigue must also be considered in the design of the joints.

When using the strained joint technique, not all combinations of materials, thicknesses, and mechanism sizes are feasible. Mechanisms using this technique are more constrained than the others that we have reviewed thus far since the panel material itself is used to realize the deflection that achieves motion. The area used for the distributed flexible joints takes away from the area used for the rigid panels; using a relatively thick and stiff material for the mechanism will require significantly larger joint areas to achieve the same folding angles than a mechanism using thinner, more flexible material. For any given combination of material and thickness there is a minimum mechanism size because, as a pattern size decreases, the ratio of joint area to panel area increases until eventually, the panels are entirely consumed by the joint areas.

Like the membrane and offset crease techniques, a key characteristic of mechanisms made with this technique is that they contain additional degrees of freedom compared to the zero-thickness reference. These extra degrees of freedom are a result of the motion and deflection possible in the compliant joints acting as surrogate folds. Because of the extra degrees of freedom, the same motion planning problems that exist with the offset crease and membrane techniques also exist with the strained joint technique. However, in another similarity to the membrane technique, the extra degrees of freedom and possible parasitic motion in the joints can be beneficial when used to accommodate thick folding of patterns that are not quite rigidly foldable or flat-foldable.

CHAPTER 3. HYBRID TECHNIQUES

This chapter introduces new hybrid approaches for accommodating-thickness in origami-inspired design. The concept of combining various thickness-accommodation techniques within a single origami-inspired-engineered system to improve overall system performance is introduced and discussed here. It is shown in this chapter that a combination of thickness-accommodation techniques can offer a better solution to origami-inspired engineering applications than a single thickness accommodation technique alone. Two ways that techniques can be combined are presented and discussed. Several hybrid technique mechanisms are presented and prototypes of them shown. This chapter is part of a recently accepted review paper about thickness-accommodation in origami-inspired engineering [4].

3.1 Combining Techniques

The concept of combining thickness-accommodation techniques was demonstrated by Lang et al. by selectively doubling hinges (doubled hinge technique) and implementing those doubled joints as SORCE joints [7]. They also discussed the possibility of combining SORCE joints with ordinary revolute joints by taking some offset functions to be zero and others to be non-zero. In this section, we expand upon those ideas introduced in [7] and show that it is possible to combine many of the thickness-accommodation techniques discussed here and that the resulting techniques offer their own unique strengths and limitations. While we do not cover every possible technique combination—obviously, the combinatorial possibilities are great—we have chosen to illustrate a few. The combinations presented here are various combinations of the rolling contact, doubled hinge, offset panel, and hinge shift techniques.

In particular, we cover two different ways that techniques can be combined: in a pattern, and at a vertex. Techniques that are combined at the pattern level we will call *hybrids*, and techniques that are combined at the vertex we will call *composites*.

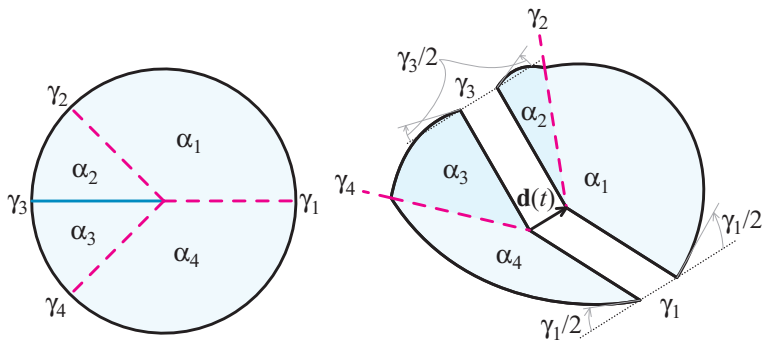

Figure 3.1: An implementation of the doubled hinge technique where the vertex is only split along the primary fold axis.

3.2 Rolling Contact/Doubled Hinge Composite

In [7], which was discussed in Section 1, a vertex that combines the technique of doubling hinges with rolling contacts was presented. We classify this vertex as composite, as it combines multiple techniques at the vertex. The doubled hinge implementation used has only two non-zero crease widths in a degree-4 vertex as illustrated in Figure 3.1. The separation distance between the split creases is not fixed, but, via rolling contacts, varies throughout the range of motion of the vertex. Once split, the modified fold pattern is translated into a thick folding mechanism by applying SORCE joints at each fold line. The advantage of using the split pattern rather than the basic SORCE concept (perpendicular motion only) is that with the addition of a dynamic split, the joint surface profiles can be more circular, thereby avoiding complex geometries.

Based upon the same bird's foot geometry, we present another variation that makes use of fixed rotational axes in combination with SORCE joints shown in Figure 3.2. By combining fixed rotational axes with rolling contact joints we are able to produce a mechanism that is self-contained within the thickness of the panels. This is an improvement over the all-SORCE configuration, which results in some of the contact joints protruding beyond the panels, as shown in Figure 3.3.

3.3 Offset Panel/Hinge Shift Hybrid

The offset panel/hinge shift hybrid technique utilizes the hinge shift technique to join offset panel units together as illustrated in Figure 3.4. While the hinge shift technique can be employed in flat-foldable degree-4, -5, or -6 configurations as shown by Chen et al., we limit our geometry to

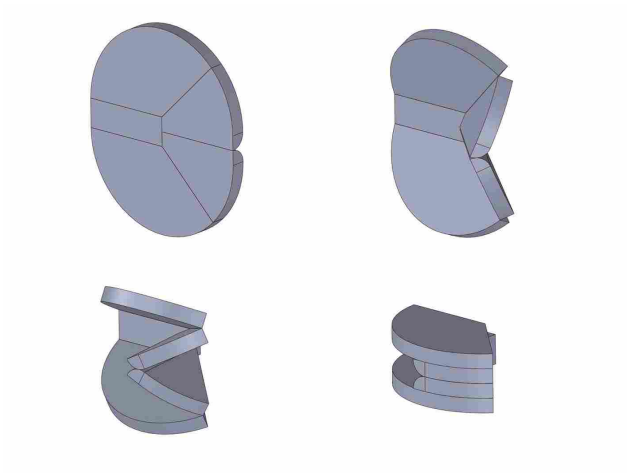

Figure 3.2: A rolling contact/doubled hinge composite vertex where traditional hinges are used together with rolling contact joints.

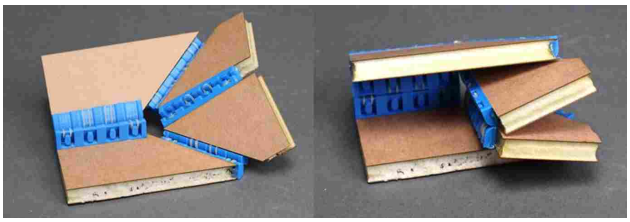

Figure 3.3: A prototype of rolling contact/doubled hinge composite vertex.

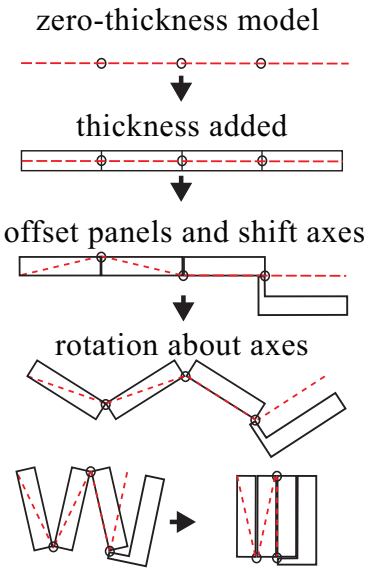

Figure 3.4: The offset panel/hinge shift hybrid technique.

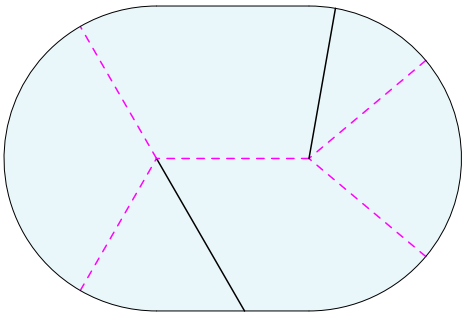

Figure 3.5: A pattern consisting of two degree-4 vertices.

the symmetric case demonstrated by Hoberman [15]. By utilizing the symmetric degree-4 vertex, the geometry of the hinge shift vertex is simplified such that hinge offsets pairs d_1 and d_3 are twice that of d_2 and d_4.

We apply the offset panel/hinge shift hybrid to a simple fold pattern consisting of two vertices, the simplest form possible for a hybrid, as shown in Figure 3.5. Note that, in this pattern, one of the vertices is symmetric to enable use of the hinge shift joint demonstrated by Hoberman and the other is an arbitrary degree-4 vertex that satisfies the flat-foldability criteria listed in Equation (2.5). We first apply the offset panel technique to the non-symmetric vertex on the right. We then use the hinge shift technique at the symmetric vertex on the left. Because the offset panel vertex shares two panels with the hinge shift vertex, the lengths of the offsets in the hinge shift vertex become twice the length they would be if employed at the first vertex due to the panel offsets of the offset panel vertex. The axis locations of the hinge shift vertex are then defined by the shared panels and axes of the offset panel vertex and Equations (2.2)–(2.4).

The resulting mechanism, as shown in Figure 3.6, is one that cannot be realized using hinge shift or offset panel technique alone. For hinge shift, only patterns such as the square twist where Equations (2.2)–(2.4) are satisfied at each vertex are possible. For the offset panel technique, this pattern would require cut-outs in some of the panels to allow otherwise intersecting offsets to pass through.

The combined offset panel/hinge shift hybrid can also solve issues that arise in the offset panel technique when dealing with tessellations (large-scale repeating patterns). In a tessellating pattern, such as the Yoshimura pattern [16], the folding/unfolding motion can go from a long flat pattern with many sections to a zero-thickness plane where all of the panels are stacked on top of

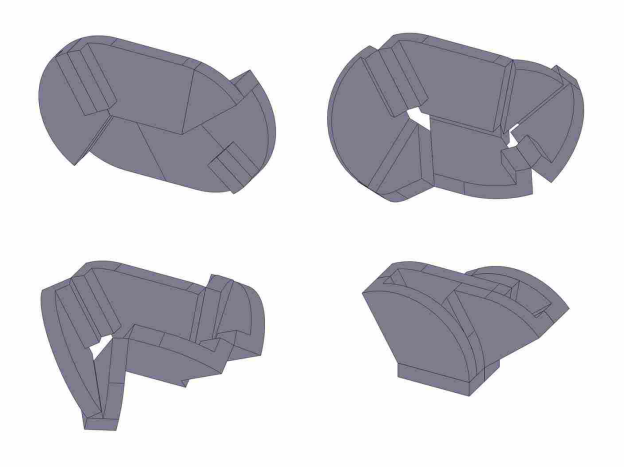

Figure 3.6: An offset panel/hinge shift hybrid mechanism.

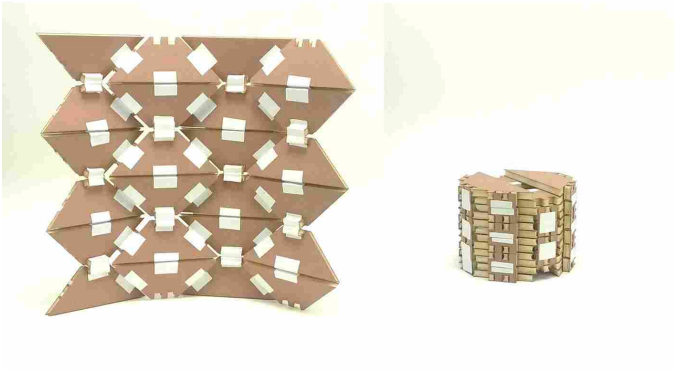

Figure 3.7: A Yoshimura pattern created using offset panel/hinge shift hybrid technique shown deployed and folded.

each other. If the offset panel technique were applied to a pattern such as this, the length of the offsets would continue to increase layer by layer, making the technique impractical when many stacking layers are involved. By using the offset panel technique in combination with hinge shift, a tessellating pattern using offset panel technique, as shown in Figure 3.7, can be realized, that scales to arbitrarily length (at least in one direction, sometimes both).

The Yoshimura pattern used in this hybrid mechanism can be realized using the hinge shift technique alone as shown in Figure 2.8. However, this is due to the symmetric nature of the pattern. In Figure 3.8, we show a prototype of a bird-base hybrid mechanism that utilizes offset panel and hinge shift, but cannot be realized using symmetric hinge shift vertices alone, and would introduce cutouts if the offset panel technique were to be used alone. It is possible that the generalized hinge

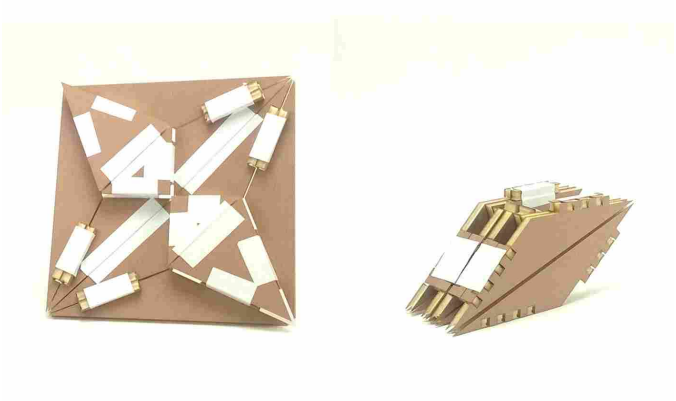

Figure 3.8: A bird-base pattern created using offset panel/hinge shift hybrid technique.

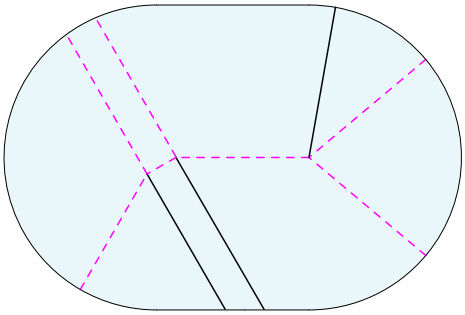

Figure 3.9: A two-vertex pattern where the left vertex has the crease doubled.

shift technique demonstrated by Chen et al. could be applied to this pattern, however, the design complexity would increase due to the non-symmetric vertices.

The bird-base pattern used in this mechanism is comprised of four non-symmetric degree-4 vertices and one symmetric degree-6 vertex. The two halves of the pattern are comprised of degree-4 vertices and each half utilizes the offset panel technique to accommodate thickness. These two halves are connected together by a single degree-6 vertex which uses the same degree-6 hinge shift vertex presented by De Temmerman [22]. It is, in total, a single-DOF mechanism.

3.4 Offset Panel/Doubled Hinge Hybrid

To illustrate the offset panel/doubled hinge hybrid, we use the same pattern shown in Figure 3.5 but split the symmetric vertex as illustrated in Figure 3.1. This pattern, shown in Figure 3.9, is now comprised of three degree-4 vertices rather than two. To combine the two techniques

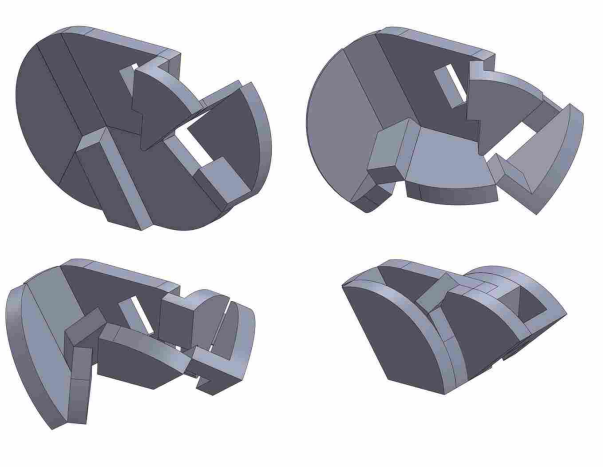

Figure 3.10: A hybrid mechanism where the right vertex utilizes the offset panel technique and the left vertex utilizes the doubled hinge technique.

together, we first begin with the doubled hinge vertex. While we could use a SORCE+doubled hinge composite for this vertex, we have decided instead to use panels for both intermediate sections and offset the panel of the mountain fold to avoid interference. The offset panel technique is then applied to the non-symmetric vertex on the right where the zero-thickness plane is determined by the doubled hinge vertex on the left. Because the hinge plane of the mechanism is driven by the doubled hinge vertex and does not lie in the middle of the panel stack of the offset panel vertex, cutouts are required for the offset panel vertex on the right.

The resulting mechanism is shown in Figure 3.10. In this generic form, any advantages of this mechanism over the one shown in Figure 3.6 are not readily apparent; discrimination between the two is going to be application-specific. Nevertheless, the fact that these two techniques can be combined gives a designer more options in the design of a thick folding mechanism.

3.5 Doubled Hinge/Hinge Shift Hybrid

We can similarly combine the doubled hinge technique with the hinge shift technique. To combine these two techniques, however, we utilize a symmetric vertex at both the left and right vertices, albeit dissimilar ones. The resulting mechanism, as shown in Figure 3.11, offers designers yet another option when considering combining thickness-accommodation techniques.

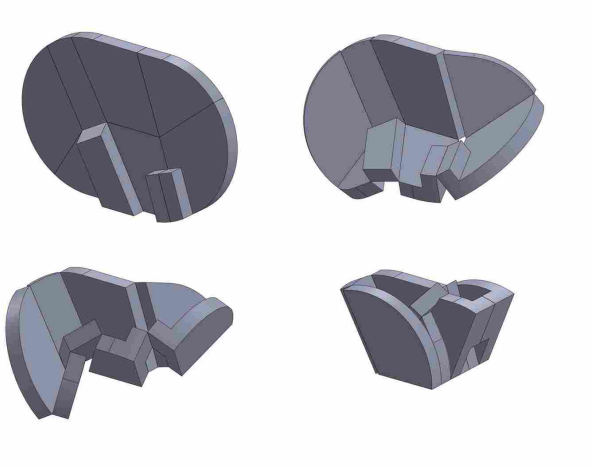

Figure 3.11: A doubled hinge/hinge shift hybrid mechanism.

3.6 Other Hybrid and Composite Techniques

Many other combinations of techniques can also be achieved. The membrane and strained joint techniques can be easily combined with other methods due to the flexibility in their motion. For example, in a thick rigid origami mechanism, part of the mechanism may not require thickness and strength and could be replaced with a thin membrane. Surrogate hinges could also be used in combination with traditional hinges. Rather than attempting to cover every possible combination—which would be combinatorially challenging—we simply present these few examples as illustration, and note that the ability for a designer to utilize different thickness-accommodation techniques at different locations within a thick origami mechanism gives them the ability to create a mechanism tailored for their specific application.

CHAPTER 4. SPLIT-VERTEX TECHNIQUE

A novel thickness-accommodation technique for origami based mechanisms is introduced in this chapter. This technique modifies a zero-thickness pattern by splitting each vertex along the minor folds into a system of two vertices. The modified fold pattern then has thickness applied to it and the resulting mechanism is kinematically equivalent to the modified fold pattern. Origami patterns that are rigid-foldable and only have two panels that stack between folds are utilized in the technique. The technique produces thick origami mechanisms where all panels lie in a plane in the unfolded state without any holes or protrusions and maintain a single degree of freedom. Steps for synthesizing split-vertex mechanisms are presented and examples of split-vertex mechanisms are shown. Advantages and potential applications of the technique are discussed. This chapter has been submitted as a conference paper and has been accepted for publication [5].

4.1 Introduction

Origami patterns have served as the basis of folding structures [22,50,51], meta-materials [52, 53], medical devices [1, 54], and space mechanisms [55, 56]. Origami is traditionally folded from paper, which is thin, and the accumulation of thickness in fold patterns generally is not an issue. In many engineering applications however, it is desirable to create folding structures out of thick materials for structural, thermal, acoustic, or other reasons. When origami mechanisms are created using thick materials, thickness accumulates and can limit the foldability of the pattern. The thick panels interfere with each-other when folded, and for the mechanism to maintain its range of motion, the issue of panel interference must be resolved.

Many thickness-accommodation techniques have been introduced which overcome the issue of panel interference in thick origami [4]. Some of these techniques maintain the original kinematic model of the flat origami pattern and address the issue of interference by either trimming the interfering edges [6], or by moving the panels away from the zero-thickness pattern via

offsets [9]. Another approach to solving the issue of interference is to use compliant hinges such as membranes [2] or surrogate folds [43] that allow the panels to distance themselves from each other in the folded state. Other approaches utilize different kinematic mechanisms than the zero-thickness model, such as sliding linkages [19], spatial linkages [15, 23], linkages where each joint of the pattern is split into two joints [33], and cam-based linkages [7]. Hybrid techniques which combine two or more techniques together have also been developed [4].

Each respective technique for accommodating thickness has a unique set of capabilities and limitations. For example, many of the alternative kinematic-linkage based thickness-accommodation techniques result in mechanisms that have holes at the vertices at some point in the folding motion. The membrane-hinge-based approach overcomes the issue of holes at vertices but lacks single-degree-of-freedom movement. The tapered-panel technique maintains single-degree-of-freedom movement while not creating holes at the vertices but panels are limited in their range of motion. By combining techniques together, new combinations of capabilities and limitations can also be achieved [4].

This paper presents and illustrates a novel thickness-accommodation technique which does not introduce holes at the vertices, and maintains the single-degree-of-freedom movement and range of motion of the zero-thickness origami pattern. This work builds upon the work presented in [32] by changing the fold pattern to introduce more folds in the zero-thickness pattern. This technique, which we will call the split-vertex technique, modifies a rigidly foldable origami pattern for thickness accommodation purposes by splitting each vertex into two vertices. The resulting patterns maintain rigidly-foldability and allow for thickness to be added without interference. The thick folding mechanisms can also be constructed such that panels do not protrude from the face of the mechanism and a perfectly flat face can be achieved. The technique has strong potential in foldable container applications or in other applications where a sealed surface is desired.

4.2 Background

An origami pattern can be seen as a system of spherical linkages where panels are links and fold lines are hinges [3]. Some origami patterns rely on the ability of paper to fold and bend not only at the creases, but in the panels as well. Rigidly-foldable origami patterns only require deflection of the creases to fold and when modeled as a linkage will have a positive mobility. In

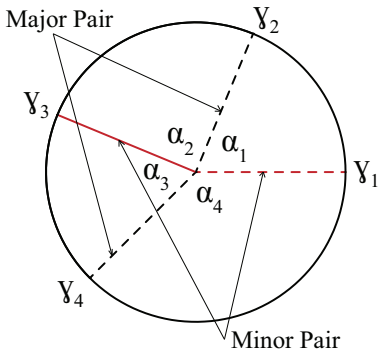

Figure 4.1: A degree 4 vertex with sector and fold angles labeled.

constructing a thick origami mechanism, it is advantageous to use rigidly-foldable patterns as most thick materials do not bend easily. For the mechanisms presented in this paper, all will be based on rigidly-foldable origami patterns.

Origami patterns are typically created from a single sheet of flat paper, a developable surface. Some patterns used in engineering applications, however, can be non-developable such as eggbox patterns [57], tube patterns [58, 59], or three-dimensional polyhedra based patterns [60]. While these patterns are useful and it is possible that the split-vertex technique could be applied to these patterns, for simplicity, we only examine developable patterns here.

The basic building block for many origami patterns is the degree-4 vertex as shown in Figure 4.1. This example vertex is comprised of three valley folds, indicated by the dashed lines, and one mountain fold indicated by the solid line. These fold lines are often grouped into two pairs which are called the minor pair and the major pair. The major pair consists of the two opposing lines that share mountain/valley assignment and the minor pair consists of the two opposing lines that have opposite mountain/valley assignment. The angle between fold lines in the pattern are called sector angles and are represented by α_1,α_2,α_3, and α_4.

A subset of origami that is of particular interest is flat foldable patterns. Flat foldablity describes an origami pattern's ability to fold into a completely flat state. In other words, all of the creases undergo 180 degrees of motion from the flat unfolded to the flat folded state. Flat foldablility is ensured by the Kawasaki-Justin theorem [61] which states that for flat-foldable vertices,

$$\alpha_1 - \alpha_2 + \alpha_3 - \alpha_4 + ... = 0. \tag{4.1}$$

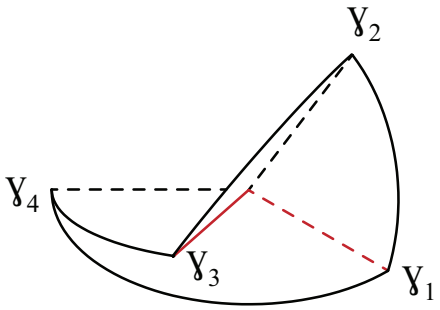

Figure 4.2: A non flat-foldable degree 4 vertex in its folded state with fold angles labeled.

For the examples presented in this paper, only flat-foldable patterns will be modified using the split-vertex technique. It is interesting to note that as we modify a flat-foldable pattern via the split-vertex technique we will convert a system of flat foldable vertices into a system of non flat-foldable vertices.

For a degree-4 vertex, the folded state may be described by the fold angles γ_1, γ_2, γ_3, and γ_4 as shown in Figures 4.1 and 4.2. These angles are the angles between the normal vectors of the sector faces. For the developable flat-foldable degree-4 vertex in Figure 4.2 the relationships between sector angles and fold angles is given by:

$$\frac{\tan\frac{1}{2}\gamma_2}{\tan\frac{1}{2}\gamma_1} = \frac{\sin\frac{1}{2}(\alpha_1+\alpha_2)}{\sin\frac{1}{2}(\alpha_1-\alpha_2)}. \tag{4.2}$$

When dealing with developable non flat-foldable vertices, such as the one illustrated in Figure 4.2, the relationships between sector angles and fold angles is more complex. These relationships have been previously derived by Huffman [62], and simplified by Lang et al. [63, Appendix A] and are:

$$\gamma_2 = 2\sin^{-1}\left[\sin(\frac{1}{2}\gamma_4)\sqrt{\frac{\sin\alpha_3\sin\alpha_4}{\sin\alpha_1\sin\alpha_2}}\right] \tag{4.3}$$

$$\gamma_1 = 2\cot^{-1}\left[\frac{\cot(\frac{1}{2}\gamma_2)(\cot\alpha_1+\cot\alpha_3)\csc\alpha_2 - \cot(\frac{1}{2}\gamma_4)(\cot\alpha_2+\cot\alpha_4)\csc\alpha_3}{\csc\alpha_3\csc\alpha_4 - \csc\alpha_1\csc\alpha_2}\right] \tag{4.4}$$

$$\gamma_3 = 2\cot^{-1}\left[\frac{\cot(\frac{1}{2}\gamma_2)(\cot\alpha_2+\cot\alpha_4)\csc\alpha_1 - \cot(\frac{1}{2}\gamma_4)(\cot\alpha_1+\cot\alpha_3)\csc\alpha_4}{\csc\alpha_3\csc\alpha_4 - \csc\alpha_1\csc\alpha_2}\right]. \tag{4.5}$$

We will use these equations to determine resulting fold angles of the spacer panels that are added as a result of splitting a vertex into two vertices.

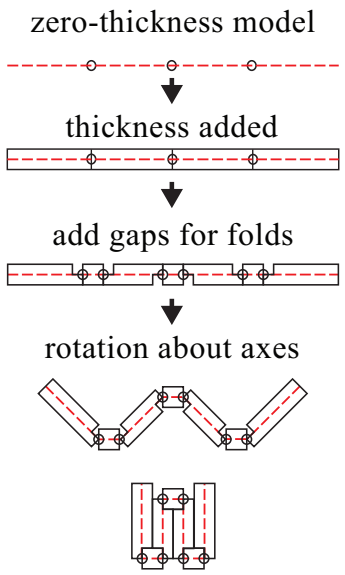

Figure 4.3: The offset-crease technique.

4.3 Split-Vertex Technique

The split-vertex technique builds upon many of the existing thickness-accommodation techniques. It bears similarity to the offset-crease technique presented by Ku et al. [32] as it introduces spacer panels at fold lines to accommodate thickness. The offset-crease technique, as illustrated in Figure 4.3, adds spacer panels at every crease or fold line. Similarly, the split-vertex technique, as illustrated in Figure 4.4, adds spacer panels, but only at select fold lines and leaves other fold lines undivided. The differences between these techniques becomes apparent at the vertex level, as shown in Figure 4.5. A degree-4 offset crease vertex is comprised of eight panels (4 sector and 4 spacer) that are connected in a loop and do not converge to a point at the center but rather there is a hole at the center to allow movement and prevent interference of the panels during folding. A degree-4 split-vertex vertex is comprised of six panels (4 sector and 2 spacer) that converge to two distinct vertices. This results in different kinematics between the offset-crease and split-vertex techniques. Offset crease degree-4 vertices are made of a 8R spatial linkage that typically has two independent degrees of freedom. A split-vertex linkage based on the same origami vertex is comprised of two spherical 4R linkages that are coupled and as a result exhibits a single degree-of-freedom. The desire to use the advantages of the offset-crease technique but to result in a single-degree-of-freedom is one motivation for the development of the split-vertex technique.

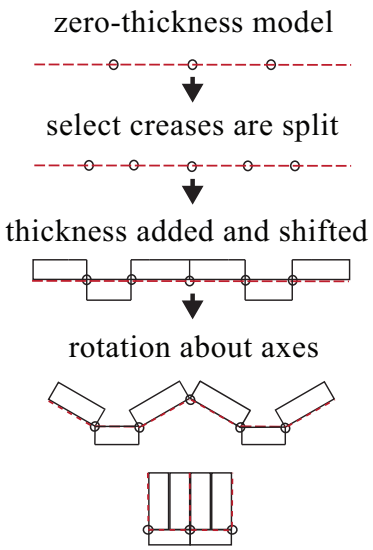

Figure 4.4: The split-vertex technique.

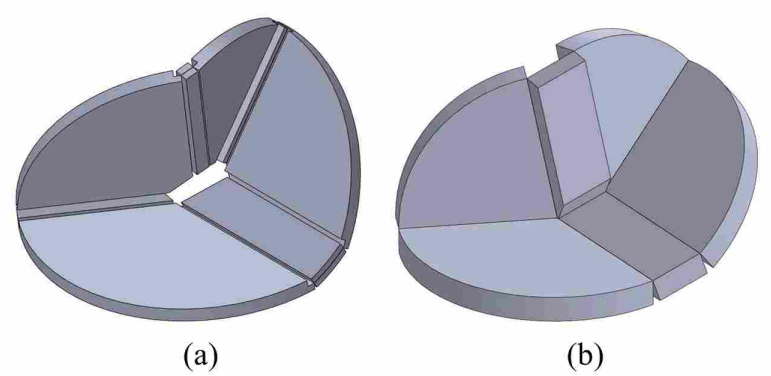

Figure 4.5: A comparison of the (a) offset-crease technique and (b) split-vertex technique for a single vertex.

Design considerations for the split-vertex technique are presented in the following subsections. For the synthesis of split-vertex mechanisms we only present the involved steps as they relate to degree-4 vertices. While it is possible that higher order vertices can be split using the same methods, as illustrated in the degree-6 vertex of the bird base pattern presented in section 4.3.6, we leave the synthesis of higher-order split vertices for future research.

4.3.1 Compatible Patterns

Determining if the origami pattern is conducive to the split-vertex technique is important because the technique does have limitations in which patterns can be accommodated. One limitation is that no more than two panels can stack between the two panels of any one fold. In other words you cannot have nesting vertices in the pattern. For a single degree-4 vertex the maximum number of panels that can stack between any one fold is two, so it can have thickness accommodated by the split-vertex technique. Origami patterns such as the bird-base pattern [32], modified Yoshimura [64], and some rigidly foldable polygons meet the criteria of only having a maximum of two panel thicknesses between any one fold in the folded state. Patterns such as the Miura-ori, where more than two panels stack between certain folds, cannot be accommodated by the methods described in this paper.

Another consideration that must be taken into account is the rigid-foldability of the split pattern. A pattern which begins as a rigid-foldable pattern, once split, may no longer be rigid foldable. This is due to the fact that a two-vertex system, once split, becomes a loop of four degree-4 vertices which is an over-constrained system that is normally not rigid foldable [65]. For the system to achieve mobility, certain geometric relationships must exist [66, 67]. To ensure that the degree-4 vertex loops created by the split-vertex technique maintain rigid-foldability, we utilize symmetry in each loop. We illustrate this idea in Figure 4.6 where a symmetric and non-symmetric two-vertex system are shown. The symmetric system, when split, will maintain rigid-foldability as long as each split line maintains symmetry as well. The non-symmetric system, however, will not be rigid-foldable when split as the degree-4 vertex loop does not have any special geometry. To ensure rigid-foldability in the split-vertex system, all the examples shown in this paper utilize symmetric origami patterns.

4.3.2 Splitting Creases

The goal behind splitting a vertex is to separate the sector panels from each other to give room for thick panels to stack. To do this we split the vertex along the fold line that has panels that stack between its adjacent panels. For a degree-4 vertex, this fold line is always one of the fold lines from the minor pair. For the vertex to maintain rigid foldability and the same panel

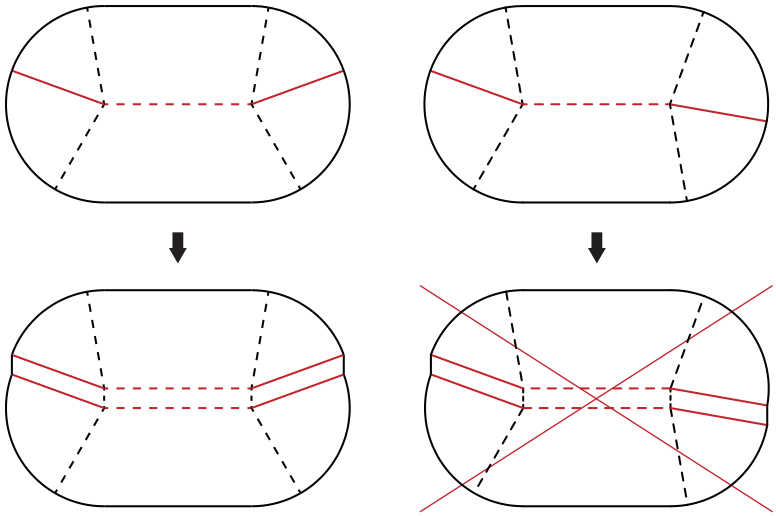

Figure 4.6: A symmetric, split-crease-compatible, two-vertex system (left) and a non-symmetric, non-compatible, two-vertex system (right).

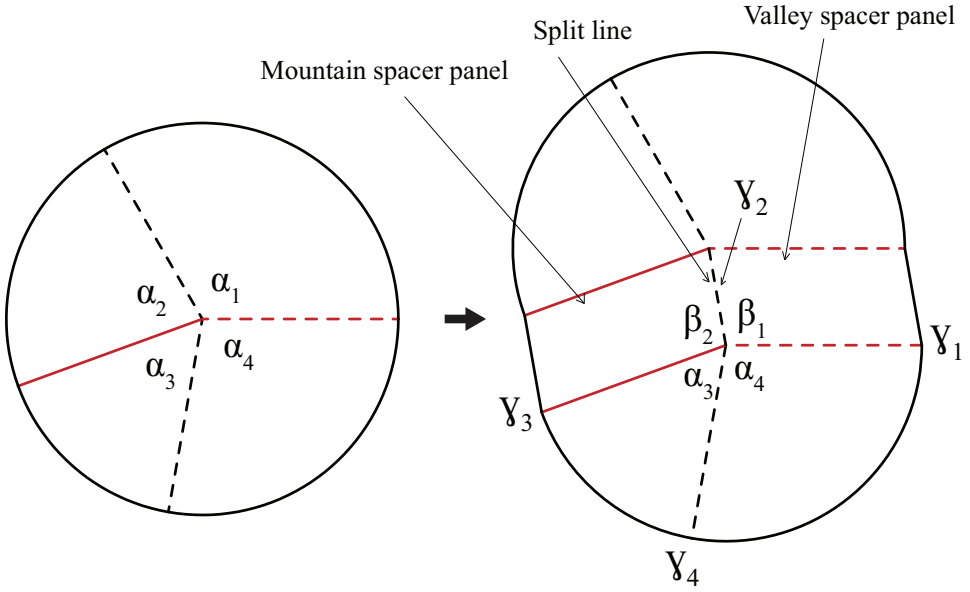

Figure 4.7: Splitting of a degree 4 vertex. Flat folding un-split single vertex (left) and split vertex with new parameters labeled (right).

geometries, we split the vertex along the minor axes and add an additional fold line that connects the two vertices. As a result two new sector panels which we will call spacer panels are created as illustrated in Figure 4.7. This creates a pair of degree-4 vertices from what once was a single degree-4 vertex.

For panel faces to fold flat against each other the lines of the new minor axis fold lines must be parallel. The distance between these lines is driven by the material thickness and the resulting fold angles of the spacer panels.

4.3.3 Split Angles

The angle of the line that connects the two vertices is called the split angle and is a parameter that can vary within a solution space and can still allow the mechanism to maintain rigid-foldability and flat-foldability for the two vertex system. This angle (β) determines the resulting fold angles of the spacer panels in the fully folded state and as a result effects the required distance of the split. The resulting fold angles are given by Equations 4.3-4.5 but now we replace α_1 and α_2 with β_1 and β_2 as shown in Figure 4.7 to distinguish the new angles formed by the split. In choosing a split angle we are mainly concerned with the resulting fold angles in the fully folded state or when γ_4 is equal to 180 degrees. Setting γ_4 equal to π and replacing α_1 and α_2 with β_1 and β_2, Equations 4.3–4.5 simplify to

$$\gamma_2 = 2\sin^{-1}\left[\sqrt{\frac{\sin\alpha_3 \sin\alpha_4}{\sin\beta_1 \sin\beta_2}}\right] \tag{4.6}$$

$$\gamma_1 = 2\cot^{-1}\left[\frac{\cot(\frac{1}{2}\gamma_2)(\cot\beta_1 + \cot\alpha_3)\csc\beta_2}{\csc\alpha_3 \csc\alpha_4 - \csc\beta_1 \csc\beta_2}\right] \tag{4.7}$$

$$\gamma_3 = 2\cot^{-1}\left[\frac{\cot(\frac{1}{2}\gamma_2)(\cot\beta_2 + \cot\alpha_4)\csc\beta_1}{\csc\alpha_3 \csc\alpha_4 - \csc\beta_1 \csc\beta_2}\right]. \tag{4.8}$$

In the split vertex, because the α sector angles are already defined, assigning one of the interior β values determines the value of the other because three of the four sector angles are now defined. The solution space for valid split angles is all angles in between where β_1 is equal to α_1 and β_2 is equal to α_2. The solution space does not contain these points, however because these points are where the introduced split line (labeled γ_2 in Figure 4.7) becomes collinear with one of the major creases and a straight-major vertex forms where it is not possible for all four creases to be partially folded at the same time [63].

In the selection of a split angle we must determine desirable outcomes by which to compare split angle selection. Desirable outcomes might include: minimum mountain spacer width,

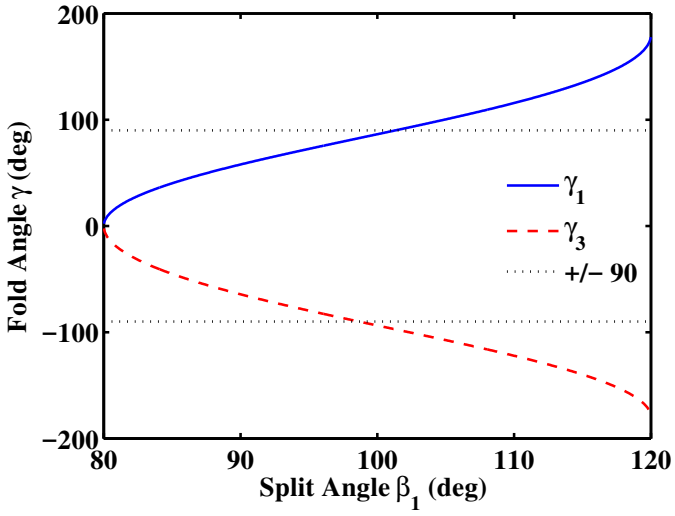

Figure 4.8: Fold angles γ_1 and γ_3 as a function of split angle β_1 for the example vertex shown in Figure 4.7.

minimum valley spacer width, or minimum combined mountain and valley spacer widths. To illustrate the trade-offs involved in choosing a split angle we will consider the vertex illustrated in Figure 4.7, a flat-foldable degree-4 vertex with a non-straight minor pair. For this particular vertex α_1=120°, α_2=80°, α_3=60°, and α_4=100°. Using Equations 4.6-4.8 we evaluate the resulting fold angles γ_1 and γ_3 which correspond to the spacer panel angles with respect to the flat parallel faces of sector panels α_1 through α_4 for all split angles β_1 in the solution space. The resulting fold angles γ_1 and γ_3 are plotted in Figure 4.8. Because the goal of splitting the vertex is to separate panels α_1 and α_2 from α_3 and α_4 by two panel thicknesses in the fully folded state, fold angles of +/- 90° will give the shortest distance between split lines, or the smallest spacer width needed, to span the gap of two panel thicknesses. The resulting fold angle in the fully flat position will also affect how much panel material needs to be removed to avoid intersection, a detail we will discuss in more depth later. In any case, the minimum amount of material that needs to be removed also occurs when the resulting fold angles are +/- 90°.

In order to identify split angle choices that result in desirable folded geometries, we define a spacer panel angle μ which represents the difference of the resulting fold angles from an ideal angle of +/- 90 degrees or:

$$\mu = \left| |\gamma| - \frac{\pi}{2} \right|. \tag{4.9}$$

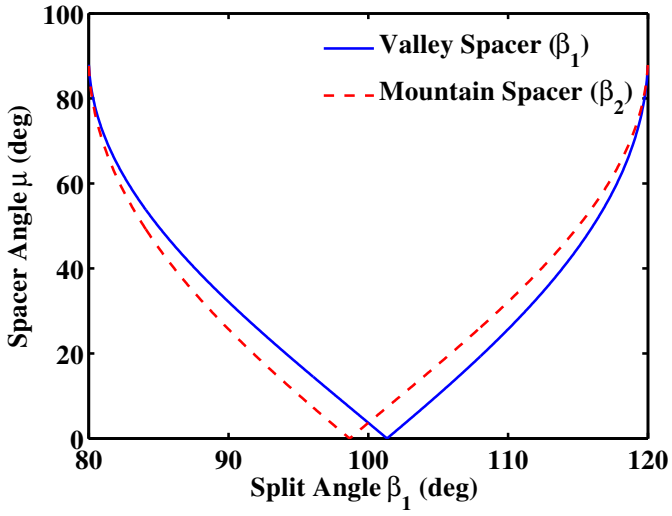

Figure 4.9: Spacer angle μ as a function of split angle β_1 for the example vertex shown in Figure 4.7.

The spacer panel angle (μ) is plotted in Figure 4.9 for this same vertex. For this vertex, and for any non-straight minor vertex for that matter, there is no split angle β_1 that will result in both spacer panels folding perpendicular to the sector panels. Instead we must choose between having a perpendicular mountain spacer (γ_3= +/-90°), a perpendicular valley spacer (γ_1= +/-90°), a solution that minimizes the difference from perpendicular spacers overall, or another solution. The angle choice that minimizes μ for both spacers is when β_1=β_2, or in terms of sector angles:

$$\beta_1 = \frac{\alpha_1 + \alpha_2}{2}. \tag{4.10}$$

In the case of a straight-minor vertex, the solution where β_1=β_2 is also the solution where both the mountain and valley spacer are perpendicular to the sector panels in the fully folded state. The straight-minor vertex is a special case that allows this. For patterns comprised of straight-minor vertices, the obvious choice for split angles is β_1=β_2=$\pi/2$.

Other factors that might influence a split angle choice may not be related to resulting spacer panel angles at all but might be related to other concerns. For example, in the bird-base pattern shown later in section 4.3.6, the split angle of β_1=90° is not chosen to minimize μ, but is chosen to

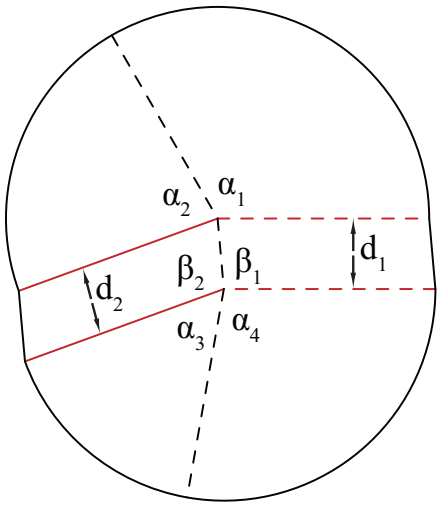

Figure 4.10: Split distances d_1 and d_2.

maintain the same sector panel sizes from the original fold pattern. For this fold pattern, the only split angle that will preserve sector panel geometries is one where all the split lines are parallel to each-other.

4.3.4 Split Distance

The split distance d is defined as the distance between each set of parallel lines in the split-vertex as illustrated in Figure 4.10. The split distance is a function of panel thickness that needs to be accommodated as well as the angle that the spacer panels form between the separated sector panels. Because each set of parallel lines is connected to each other through the two vertices, given a split angle β_1 or β_2, if one split distance is specified (d_1 or d_2) then the other is a function of that split distance and the split angle.

To determine the required distance between split lines we must first know the spacer panel angle μ for both the mountain and valley spacers. If both the mountain and valley spacer have the same μ value ($\beta_1 = \beta_2$) then $d_1 = d_2$ and their distance required to accommodate panels with a uniform thickness of t will be

$$d = \frac{2t}{\cos(\mu)} = 2t\sec(\mu). \tag{4.11}$$

We note that as the spacer panel angle μ approaches $\pi/2$ the spacer width d goes to infinity. This illustrates why it is desirable to keep μ to a minimum.

When the split angles β_1 and β_2 are not equal then the split distances d_1 and d_2 will have different values and will have to be evaluated independently. Because each distance can be written as a function of the other distance and the sector angles, the corresponding distances for each split distance are also evaluated. The largest distance must then be selected to accommodate two panel thicknesses.

4.3.5 Addressing Intersection

After modifying the fold pattern to accommodate the stacking of thick panels, we then add thickness to the pattern. Adding thickness uniformly to one side of the pattern will cause interference in the folding motion. To address panel intersection we employ two methods: shifting panel thickness, and trimming panel edges. The first method as illustrated in Figures 4.4 and 4.5b shifts the mountain or valley spacer panels (depending on which side thickness is added) to the opposite side of the zero thickness reference plane. The second method as illustrated in Figure 4.11 keeps the thickness on the same side of the zero thickness reference plane and trims the corners that would interfere when folded. This method uses the same approach of the tapered panel technique described in [6]. An advantage of applying the split-vertex technique before trimming interfering edges is that much less material needs to be trimmed and only certain edges require trimming while others do not.

When the first method is used, a subsequent step of the second method may also be required. Such is the case with the vertex shown in Figure 4.5b. The mountain spacer which has been shifted to the opposite side of the zero-thickness reference plane would intersect with the valley spacer when fully folded. To avoid this, the inside edge has been trimmed the amount that would otherwise intersect. Non-straight minor vertices would also require a subsequent trimming step if the panel thickness shift technique were used, as the spacer panels do not end up perpendicular to the sector panels and because of the spacer panel angle, one of the spacer panel edges would interfere with the sector panels.

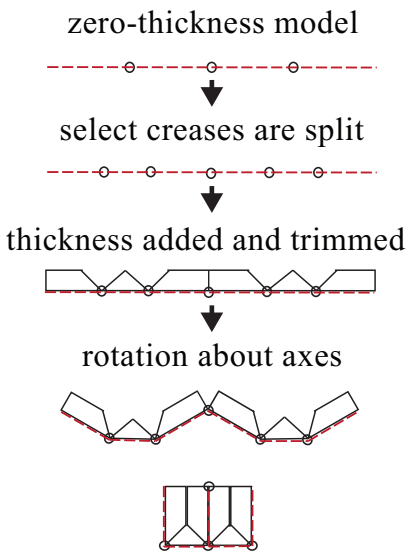

Figure 4.11: Split-vertex technique with alternative interference accommodation method.

4.3.6 Applying the Split-Vertex Technique

Although a single vertex mechanism can be useful on its own, the majority of origami-based engineering applications utilize folding patterns comprised of multiple vertices. We present in this section several examples of thick origami mechanisms that can be created using the split-vertex technique.

The first example is that of a rigidly foldable hexagon twist shown in Figure 4.12. This pattern is based on rigidly foldable twist work presented in [68]. The minor folds in this pattern are highlighted in red. We then split the vertices along the minor folds and add a connecting split line. For the split angle in this pattern we choose and an angle such that $\beta_1 = \beta_2$, minimizing the required width of the spacers. We then calculate the width of the spacers from Eq. 4.11 based on the chosen panel thickness and add thickness to the pattern.

We note that for the pattern to maintain the same sector angle relationships, some of the edge lengths of the exterior panels change as a result of adding the spacer panels. Intersecting edges are then trimmed and the mechanism folds as shown in Figure 4.13. Because all of the hinges of the mechanism lie on the flat top face of the mechanism, and all the tapered and cut edges are on the backside of the mechanism, this technique is ideal for fabrication by machining. A hexagon prototype machined out of polypropylene is shown in Figure 4.14. The prototype achieves motion

through the use of living hinges which are machined into a solid piece of polypropylene. Pockets are also machined out of the back of the panels to reduce weight but maintain stiffness.

The second example is the bird base pattern shown in Figure 4.15. This pattern is comprised of degree-4 vertices as well as one degree-6 vertex in the center. For the degree-6 vertex we split it along the mountain fold to give room for the surrounding sector panels to stack. The other vertices are split along the minor fold creases. For the split angles in this pattern, instead of choosing fold angles that minimize the width of the spacer panels we choose a fold angle $\beta_1 = 90^\circ$ that maintains the same edge lengths of the exterior panels. This results in all of the split lines being parallel with each other. A prototype of this mechanism is shown in Figure 4.16.

Other patterns that have been explored using the split-vertex technique include the rigidly foldable square patterns shown in Figure 4.17. The mechanism at the top of Figure 4.17 is a square-twist-based fold pattern similar to the hexagon twist shown in Figure 4.13, the difference being number of sides of the central polygon. Any even-number-sided polygon can be constructed in a similar manner. The mechanism shown at the bottom of Figure 4.17 is a square-twist pattern with straight-major fold pairs. This pattern simply becomes a grid where each fold is folded independent of the others. The split-vertex technique is able to accommodate thickness in straight-major fold patterns whereas some thickness-accommodation techniques cannot.

4.4 Discussion

The split-vertex technique offers several advantages as a thickness-accommodation technique. One advantage is the ability for the pattern to lay completely flat without holes or height variations on the upward facing surface. Another advantage is that the mechanism retains its single-degree-of-freedom movement. While some techniques maintain a smooth flat surface, and others maintain single DOF movement, thickness-accommodation techniques to date have not been able to achieve both criteria. This makes the split-vertex technique an appropriate thickness-accommodation technique for applications where a smooth surface without holes and single-degree-of-freedom movement is important. Table 4.1 compares some of the attributes of the split-vertex technique with existing techniques. The main disadvantage of the split vertex technique is that it cannot be applied to arbitrary fold patterns. The axis-shift technique also cannot be applied to arbitrary patterns but the fold pattern geometry requirements are different for it than for the split-

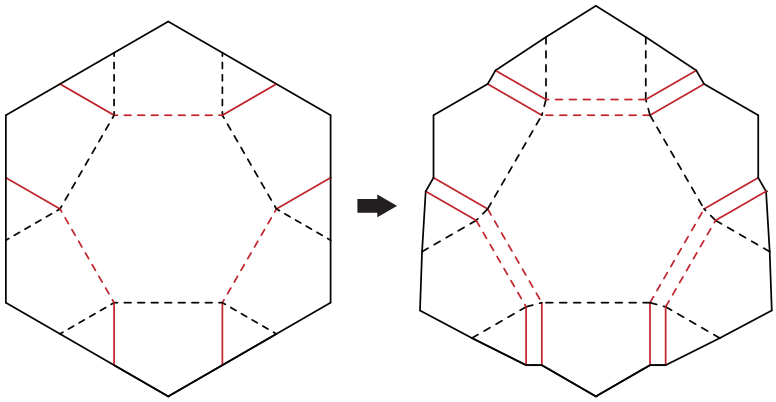

Figure 4.12: Split-vertex technique applied to hexagon pattern.

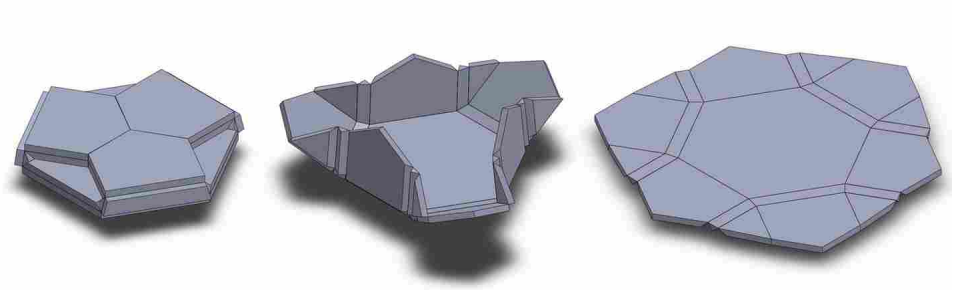

Figure 4.13: CAD model of split-vertex hexagon pattern going through folding motion.

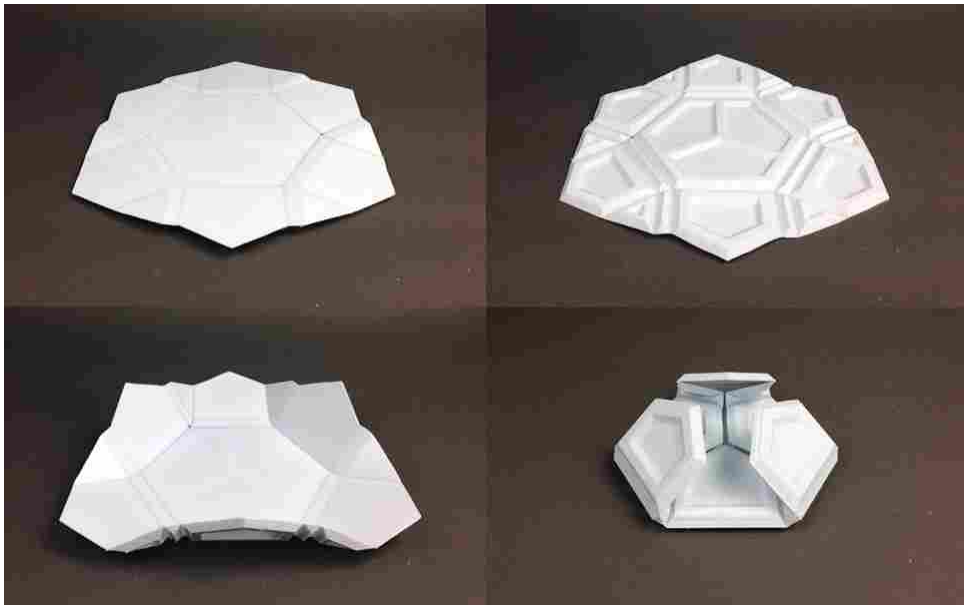

Figure 4.14: Monolithic prototype of split-vertex hexagon pattern machined out of polypropylene.

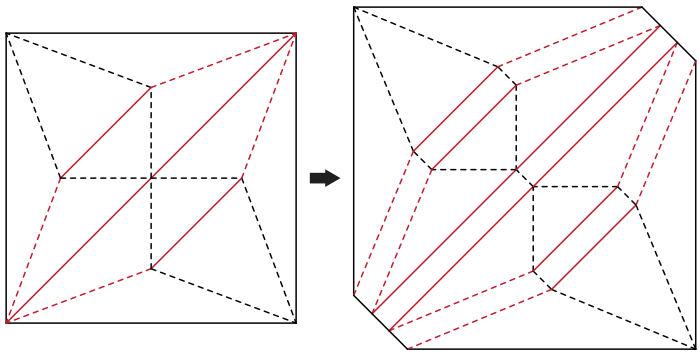

Figure 4.15: Split-vertex technique applied to bird base pattern.

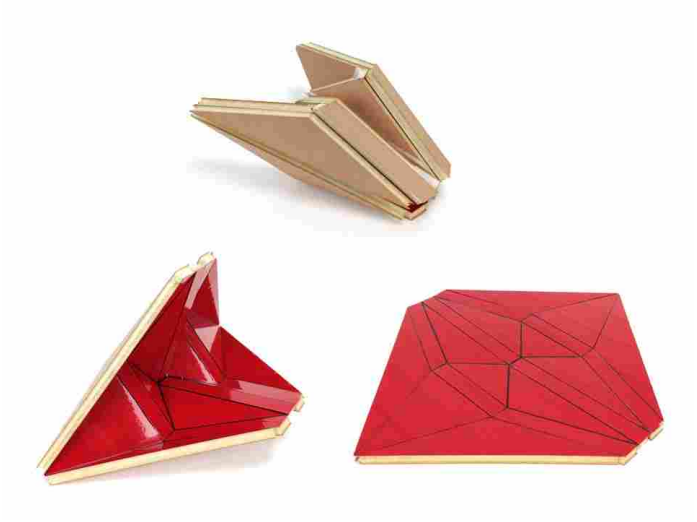

Figure 4.16: Prototype of split-vertex bird base thick origami mechanism fabricated from foam board and red polypropylene tape, demonstrating a flat surface with no holes.

Table 4.1: Comparison of different attributes of some thickness-accommodation techniques.

	Arbitrary Patterns	Single DOF	Flat Surface	No Holes
Axis Shift		X		
Offset Panel	X	X		
Tapered Panel	X	X		X
Offset Hinge	X		X	
Rolling Contact	X	X		
Membrane Folds	X		X	X
Strained Joint	X		X	
Split-vertex		X	X	X

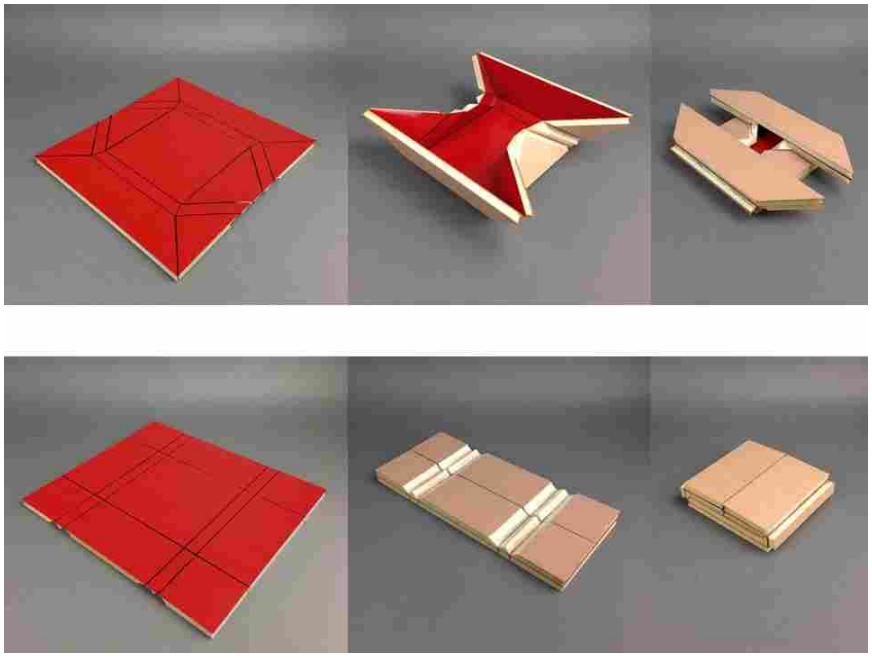

Figure 4.17: Rigidly-foldable square patterns realized using the split-vertex technique. Top: square twist based fold pattern. Bottom: straight-major square-twist pattern. The red surface demonstrates the ability to create a flat surface with no holes.

vertex technique. For the axis-shift technique a certain sector angle, axis shift distance relationship must be maintained for the mechanism to achieve mobility. This same sector angle relationship does not apply to the split-vertex technique but fold patterns that have nesting vertices cannot be accommodated.

The split-vertex technique is a promising technique for applications in folding containers or products where a folding mechanism with no holes is desired. Because the technique does not require offsets or hinges located on different faces, split-vertex mechanisms can be fabricated from sheet materials. Monolithic mechanisms that utilize living hinges can also be fabricated by machining or removing material on one side of the sheet.

4.5 Conclusions

A novel thickness-accommodation technique, the split-vertex technique has been presented and discussed. The technique offers the advantage of accommodating thickness without introducing holes or protrusions in the mechanism while maintaining single-degree-of-freedom kinematics. The technique is applicable to patterns comprised of degree-4 vertices where vertices do not nest

inside of each other. The technique is also able to accommodate straight-major fold patterns. The technique shows promise in applications where a sealed surface must be maintained such as in collapsible containers or shelters. The flat construction of split-vertex mechanisms lend themselves well to planar fabrication techniques. More work can yet be done in applying the split-vertex technique in engineering applications.

CHAPTER 5. THICKNESS-ACCOMMODATION IN NON-DEVELOPABLE ORIGAMI

This chapter introduces the use of thickness-accommodation techniques for non-developable origami patterns. Thickness-accommodation techniques have been developed in the context of developable origami patterns. While most origami patterns are developable, many useful patterns exist which are non-developable. Methods for applying thickness-accommodation techniques to non-developable origami patterns are discussed. For spherical-mechanism-based techniques, few if any changes to the technique are needed to apply to non-developable patterns. For spatial-mechanism-based techniques, additional constraints must be taken into account. Example non-developable thick-origami mechanism are discussed and prototypes are shown.

5.1 Introduction

Origami has served as inspiration in a wide range of engineered systems including folding structures, space mechanisms, medical devices, and consumer products. Characteristics of origami that are often exploited in these applications include shape transforming behavior, single sheet construction, kinematic motion, and aesthetic appeal. The use of paper in origami has resulted in patterns with desirable attributes including the ability of a large pattern to stow compactly, simple manufacturing, low cost construction, and the ability to create curved crease patterns. While paper as a material is suitable in art and some engineering applications, the majority of engineering applications require materials that are stronger, stiffer, and can withstand harsh environments. In many cases it is desirable to use thick materials for increased stiffness and strength. When thickness is introduced in an origami-based mechanism, that thickness must be accommodated for to prevent self intersection of panels. Many techniques have been introduced which accommodate for thickness in origami-based mechanisms.

When designing origami-inspired engineered systems, some of the traditional characteristics of origami can be disregarded. One example is that of developability. A developable surface, or

a Euclidean surface, is one where double curvature does not exist and can be flattened into a plane without stretching of the material. Because origami starts with a flat sheet of paper and is folded into a 3D shape, it can likewise be unfolded back into a flat sheet and is therfore developable. Although cutting and gluing is typically eschewed in origami, in engineering design some interesting and useful designs have come about by cutting and gluing paper, including eggbox patterns [57], tube patterns [58, 59], and three-dimensional polyhedra based patterns [60].

Thickness accommodation techniques have been applied primarily to developable patterns. This work seeks to expand the scope of many thickness accommodation techniques to include patterns that are non-developable. Additional considerations that must be made when dealing with non-developable thick origami and the constraints that some techniques have with non-developable vertices will be discussed.

5.2 Background

The basic building block for many origami patterns is the degree-4 vertex as shown in Figure 5.1. This example vertex is comprised of three valley folds, indicated by the dashed lines, and one mountain fold indicated by the solid line. These fold lines are often grouped into two pairs which are called the minor pair and the major pair. The major pair consists of the two opposing lines that share mountain/valley assignment and the minor pair consists of the two opposing lines that have opposite mountain/valley assignment. The angle between fold lines in the pattern are called sector angles and are represented by α_1,α_2,α_3, and α_4. The angles that the panels of vertex form with each other are called fold-angles and are represented by γ_1, γ_2, γ_3, and γ_4.

An origami pattern can be seen as a system of spherical linkages where panels are links and fold lines are hinges [3]. Some origami patterns rely on the ability of paper to fold and bend not only at the creases, but in the panels as well. Rigid-foldable origami patterns only require deflection of the creases to fold, and when they are modeled as linkages have positive mobility.

A subset of origami that is of particular interest is flat foldable patterns. Flat foldablity describes an origami pattern's ability to fold into a completely flat state. In other words, all of the creases undergo 180 degrees of motion from the flat-unfolded to the flat-folded state. Flat fold-

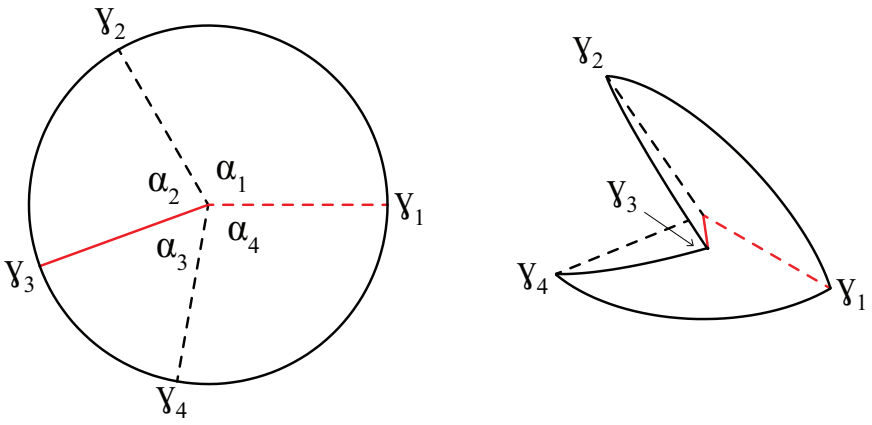

Figure 5.1: A developable degree-4 vertex in its unfolded state (left) and partially folded state (right).

ablility is ensured by the Kawasaki-Justin theorem [61] which states that for flat-foldable vertices,

$$\alpha_1 - \alpha_2 + \alpha_3 - \alpha_4 + ... = 0. \tag{5.1}$$

5.3 Non-developable origami

Although definitions for non-developable vertices have been assigned in various research fields, we limit the definition of a developable origami vertex to one that can only fold flat without any cutting. In other words the sector angles of a developable origami vertex must sum to 2 π. If the sum of the sector angles is less than 2π we call the vertex *under-developed*, and if the sum is greater than 2π we call the vertex *over-developed*. An under-developed vertex is still developable in mathematical terms by means of cutting and flattening, however an over-developed vertex is not developable, even with cutting and flattening because when the vertex is flattened there is overlap of the sector edges which makes it impossible to fabricate from a single planar medium [69]. Example under-developed and over-developed vertices are shown in Figures 5.2 and 5.3.

It is interesting to note that on both the under-developed and over-developed vertices, one of the creases of the major crease pair changes from mountain to valley assignment throughout the folding motion. The behavior of under-developed and over-developed vertices can be quite different than developable vertices and is an area that warrants further research.

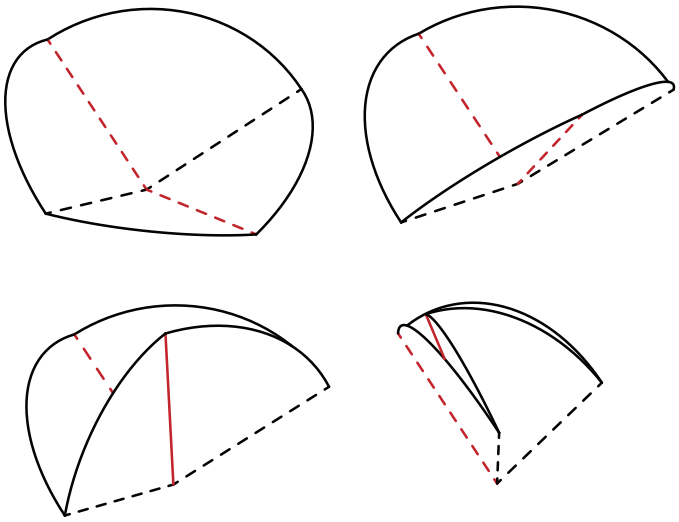

Figure 5.2: An under-developed degree-4 vertex going through its folding motion.

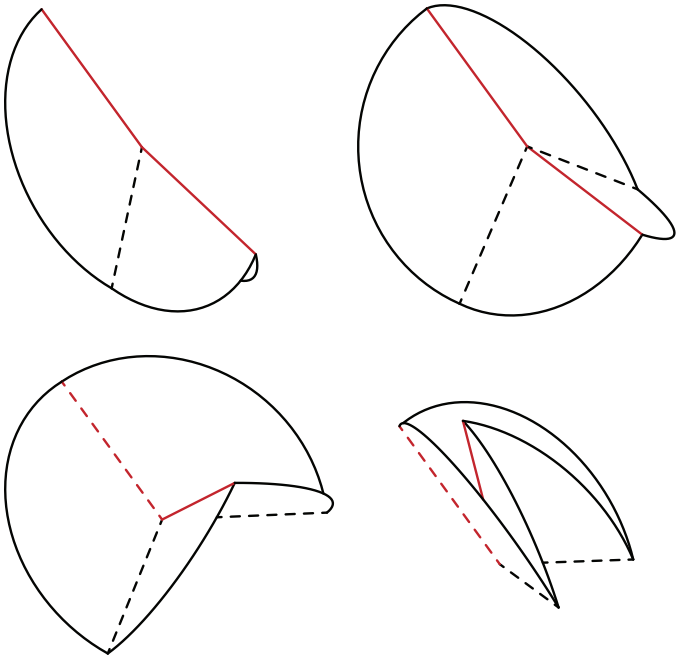

Figure 5.3: An over-developed degree-4 vertex going through its folding motion.

5.4 Non-developable Thick Origami

It is desirable to apply thickness-accommodation techniques to non-developable patterns because most engineering applications of origami require the use of materials with non-negligible thickness. Because the majority of origami patterns are developable patterns, thickness-accommodation techniques have been developed in the context of developable patterns.

Because thickness-accommodation techniques utilize different mechanisms in their construction, (e.g. spherical linkages and spatial linkages), transitioning from a developable pattern to a non-developable affects the techniques differently. These differences are discussed in this work.

In engineering applications of non-developable origami, patterns such as tubes [58] and egg-box patterns [57] have been found to have promising potential in structures. These patterns along with other non-developable patterns are used here to demonstrate the application of thickness-accommodation techniques to non-developable origami.

5.4.1 Tapered and Offset-Panel techniques

The spherical linkage utilized in the tapered-panel and offset-panel techniques is the same mechanism used in the zero-thickness origami pattern. Because the spherical linkage applies to under-developed, over-developed, and developable vertices, the transition from a developable thick origami mechanism to a non-developable thick origami mechanism is simplified. Changes that occur in the zero thickness mechanism also occur in the thick-origami counterpart. The same steps used to create a developable-thick-origami mechanism can be followed with a non-developable pattern. In Figures 5.4 and 5.5 the offset panel technique is shown applied to an under-developed hexagon pattern and an under-developed box pattern.

5.4.2 Axis-shift technique

The axis-shift technique shifts the hinge lines rather than the panels of a zero-thickness pattern to accommodate thickness. An example degree-4 axis-shift vertex is illustrated in Figure 5.6. As seen in this figure, because the hinge lines have been shifted, they no longer lie in the same plane when folded flat and they no longer intersect at a point throughout the folding motion. This the linkage is no longer a spherical mechanism but is a spatial 4-R mechanism known as the

Figure 5.4: An under-developed hexagon pattern modified using the offset-panel technique.

Bennett Linkage, where opposing link pairs are equal in length and have the same rotational axis twist. The criteria for the mechanism to achieve mobility are [23]:

$$\alpha_1 + \alpha_3 = \alpha_2 + \alpha_4 = \pi \tag{5.2}$$

$$d_1 = d_3, d_2 = d_4 \tag{5.3}$$

$$\frac{d_1}{d_2} = \frac{\sin(\alpha_1)}{\sin(\alpha_2)} \tag{5.4}$$

The first criteria listed in Equation 5.2 corresponds with the flat foldability criteria given in Equation 5.1. This means patterns modified with the axis-shift technique must be flat foldable to achieve mobility. Another consequence of Equation 5.2 is that the sum of all the sector angles α_1 through α_4 must equal 2π. This means that the axis-shift technique for degree-4 vertices as discussed in [23] is only applicable to developable origami patterns.

The spatial 4R linkage equations given by Chen et al. [23] only apply to developable vertices. This linkage discussed in [23] however, is a special case of the general Bennett linkage. The

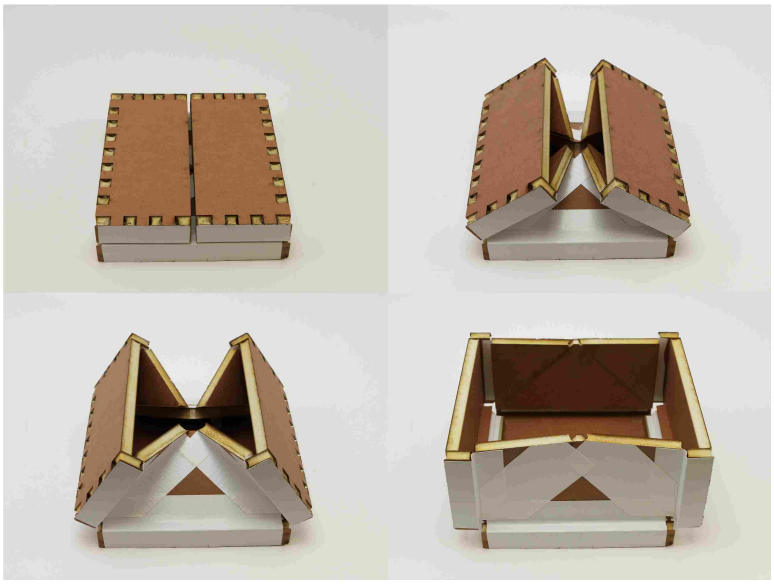

Figure 5.5: An under-developed box pattern modified using the offset-panel technique.

general Bennett linkage equations are the same as listed above, however equation 5.2 in its general form is:

$$\alpha_1 + \alpha_3 = \alpha_2 + \alpha_4. \tag{5.5}$$

The traditional Bennett linkage is often described as having opposing links that are equal in length and have equal twist angles. However, the linkage in [23], as shown in Figure 5.7, does not share the same twist angle on opposing links but opposing link pairs are compliments. Because opposing twist angles are compliments, the sum of the twist angles must equal 2π, constraining origami mechanisms of this type to developable patterns.

The traditional Bennett linkage as shown in Figure 5.8 has opposing link pairs that are equal in length and share the same twist angle. Because the panel sector angles of this linkage are greater than $\pi/2$, the sum of the sector angles is greater than 2π, resulting in an over-developed vertex. A singularity where only two links can achieve mobility arises in this mechanism when it is developable, i.e. when sector angles equal $\pi/2$. Because of this, the traditional Bennett linkage only applies to non-developable origami patterns whereas the compliment-type Bennett linkage only applies to developable origami patterns.

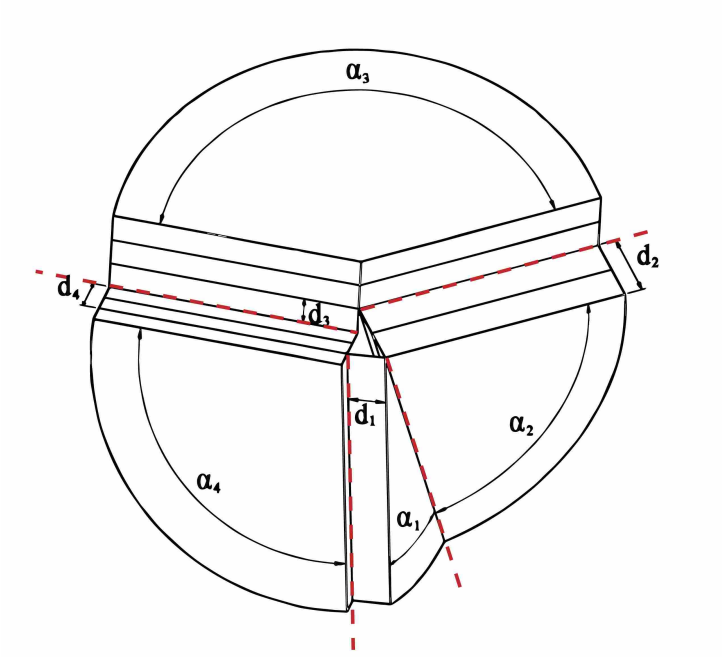

Figure 5.6: An example axis-shift vertex. Hinges are indicated by red dashed lines.

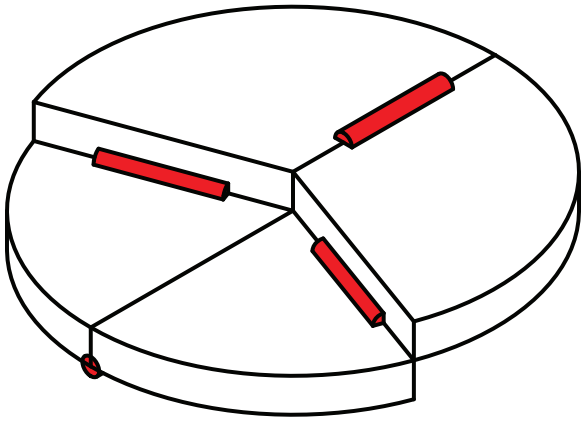

Figure 5.7: A symmetric-compliment-type Bennett linkage where opposing twist angles are not equal but are compliments.

To show example applications of the non-developable-type Bennett linkage we apply the axis-shift technique to origami tube patterns and egg-box patterns. An optimization of the geometry of these thick origami tubes is discussed in [70]. A symmetric thick tube design is shown in Figure 5.9. This tube is comprised of under-developed, developable, and over-developed vertices. The Bennett linkage is applied to all vertices, the compliment-type to the developable vertex,

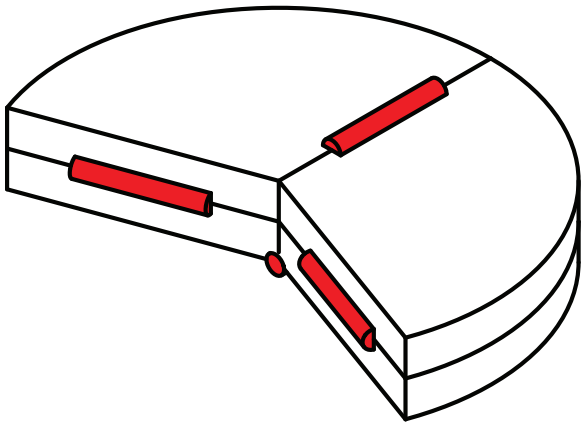

Figure 5.8: A symmetric Bennett linkage where opposing links have equal lengths and twist angles.

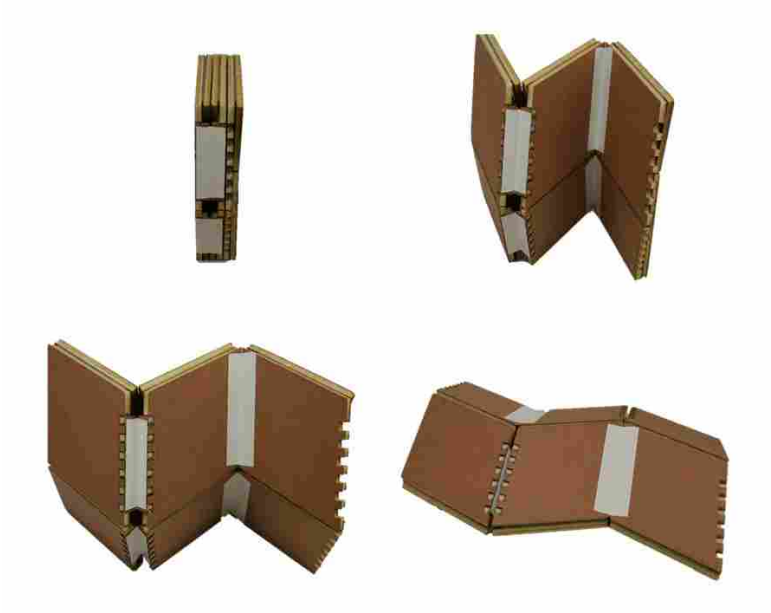

Figure 5.9: Foam-board prototype of symmetric-non-developable-thick tube.

and the traditional-type to the over-developed and under-developed vertices. These three different types of vertices of the tube are shown in Figure 5.10.

In [70] a non-symmetric thick tube as shown in Figure 5.11 is discussed. Because of the non-symmetric geometry of this tube, Bennett linkages cannot be utilized at the vertices. To overcome the constrained geometry of this tube, two degree-4 vertices are replaced with a single 6R Bricard linkage [71]. This higher-order linkage provides the extra degrees-of-freedom needed to achieve mobility. The resulting mechanism maintains a single degree of freedom.

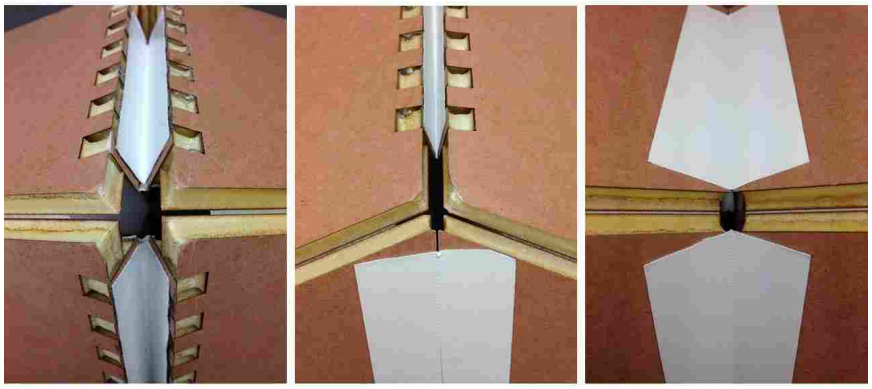

Figure 5.10: The three different linkages used in the symmetric-thick-origami tube. Left: an under-developed-traditional-Bennett linkage. Center: a developable compliment-type Bennett linkage. Right: an over-developed-traditional-Bennett linkage.

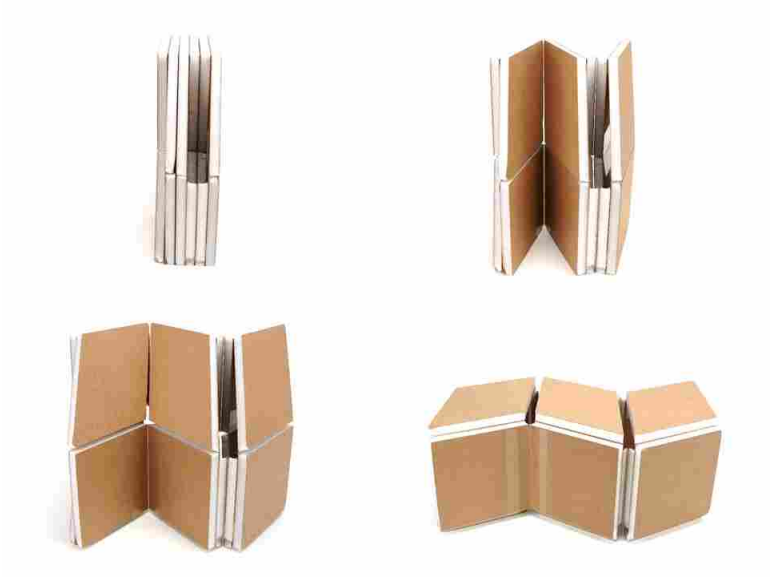

Figure 5.11: Foam-board prototype of non-symmetric non-developable-thick tube.

We also apply the axis-shift technique to the non-developable-egg-box pattern and egg-box-inspired-tube pattern shown in Figures 5.12 and 5.13. These patterns consist of over-developed and under-developed vertices. For the over-developed vertices, traditional Bennett linkages are utilized and for the under-developed vertices, under-developed-spherical linkages are used.

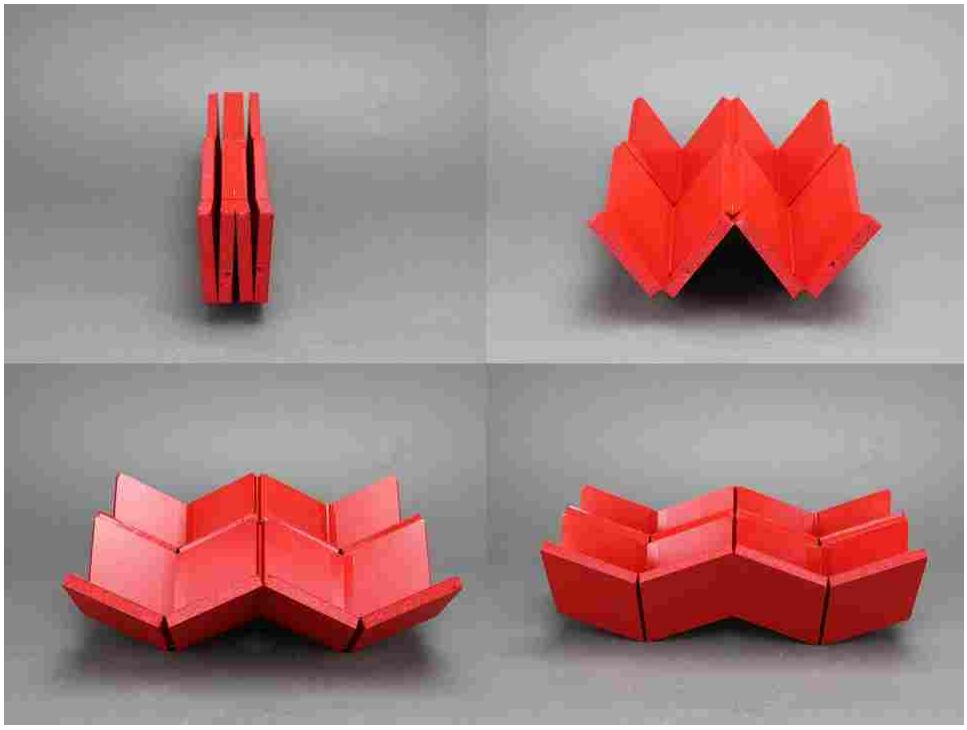

Figure 5.12: Eggbox pattern comprised of over-developed Bennett linkages and under-developed spherical linkages.

5.4.3 Split-vertex technique

The split-vertex technique shows much potential in non-developable-origami applications. Because this technique utilizes spherical linkages like the tapered-panel and offset-panel techniques, the technique does not have the constraints of the axis-shift technique. The application of the split-vertex technique to non-developable patterns, however, is more complex than the tapered-panel or offset-panel technique because symmetry must be maintained in the split-vertex loop. The fold angle of the spacer panel must also be taken into consideration to design optimum configurations.

The sector-angle and fold-angle relationships given in [5] are for developable vertices. To derive these relationships for non-developable vertices is more complex [63]. One way to avoid these complexities is to begin with a non-developable pattern that utilizes symmetric-degree-4 vertices. As discussed in [5] the splitting of a symmetric-degree-4 vertex is the only case where a minimum-width spacer panel can be used and is the easiest case to design.

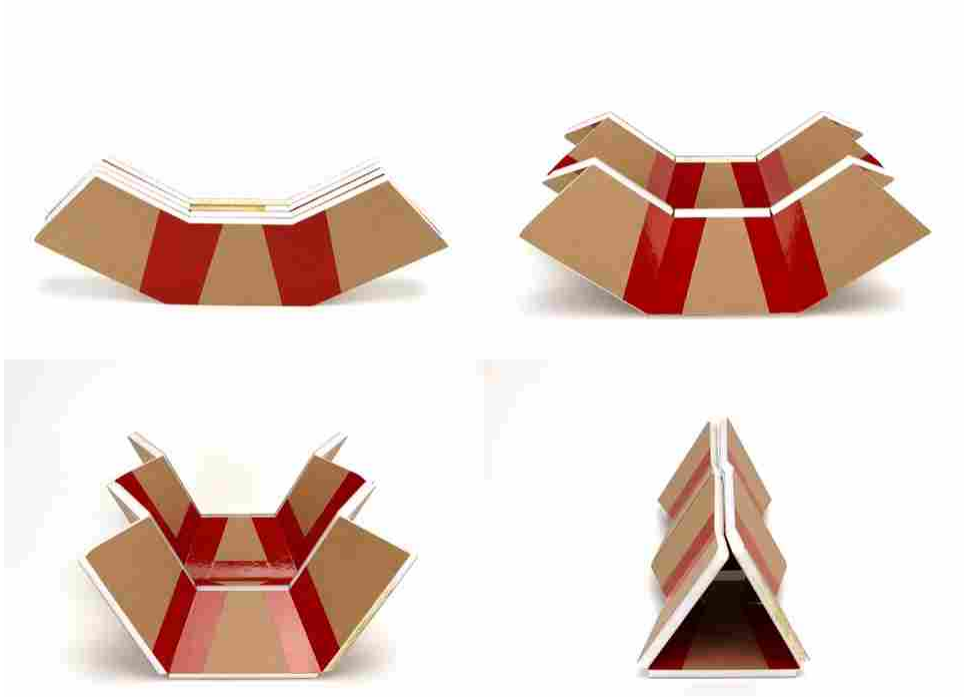

Figure 5.13: Eggbox inspired non-developable tube comprised of excess-vertex Bennet linkages and deficient-vertex spherical linkages.

The application of the split-vertex technique to a under-developed-hexagonal bowl is shown in Figure 5.14. This pattern uses symmetric vertices to simplify the design. An interesting bi-product of the split-vertex technique applied to non-developable patterns is that the spacer panel acts as a chamfer between the neighboring panels. This has a smoothing effect on the geometry and can be seen in the hexagonal bowl shown in Figure 5.14. This makes the bowl geometry smoother on the inside surface. The split-vertex technique applied to non-developable origami patterns has great potential in folding packaging, or container applications where the deployed shape is often non-developable and a sealed inside surface is required.

5.5 Conclusions

This work has shown how thickness-accommodation techniques can be applied to non-developable origami patterns. The Bennett linkage for non-developable and developable applications has been discussed in detail. Examples of non-developable thick origami mechanisms have

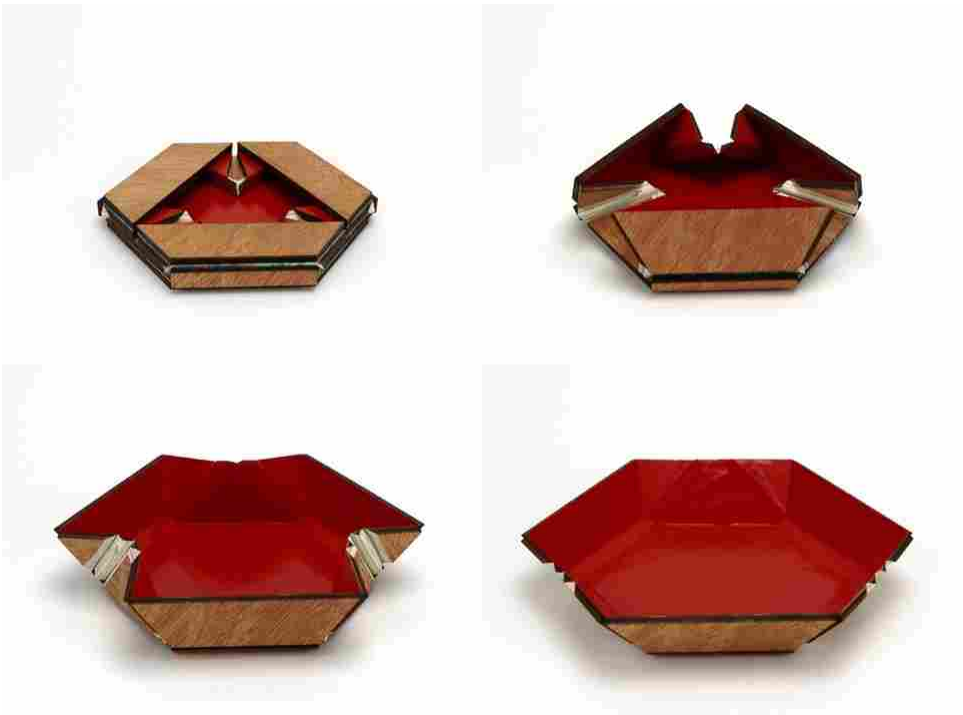

Figure 5.14: Split-vertex implementation of a non-developable hexagon pattern.

been demonstrated here using the offset-panel technique, axis-shift technique, and split-vertex technique. While other existing thickness-accommodation techniques could also be applied to non-developable origami patterns we leave this area for future research. Non-developable-thick origami mechanism have potential for applications in various origami-inspired engineered systems.

CHAPTER 6. DESIGN OF AN ORIGAMI-INSPIRED DEPLOYABLE AERODYNAMIC LOCOMOTIVE FAIRING

The design of an aerodynamic origami-inspired deployable fairing for locomotives is discussed in this chapter. Because freight locomotives may or may not be in the lead position and the constrained space between coupled locomotives is small, it is desirable for the fairing to be stowed flat in the non-lead position. The fairing is based on non-developable thick origami. Thick origami has traditionally only been applied in the context of developable patterns. Considerations for applying thick origami to non-developable patterns is discussed. The fairing geometry is optimized using CFD analysis and multi-dimensional polynomial regression. Prototypes of the fairing are constructed to validate its operational feasibility. The fairing is estimated to reduce overall aerodynamic drag on the locomotive by 16% at a 80 kph velocity. This translates into an estimated fuel savings of over $2,000,000 a year per fleet of 1,000 trains.

6.1 Introduction

Aerodynamic drag is one of the largest contributing factors to the fuel consumption of large vehicles at cruising speed. Large freight vehicles would benefit from aerodynamic improvements in their design but are often constrained by functional requirements such as accessibility and overall size.

Origami has been used as a source of inspiration in solving some of the most difficult space constrained problems ranging from space [55] to medical applications [72]. This project utilizes the principals of origami to create a transformable aerodynamic add-on device for locomotives. The device, which we will refer to as the fairing, can transform its shape from an aerodynamic form to a collapsed form so that the functional requirements of the locomotive is maintained. The basic concept of this reconfiguration is shown in Figure 6.1. The deployed configuration is meant to decrease pressure drag on the lead locomotive of a train. The stowed configuration is meant to

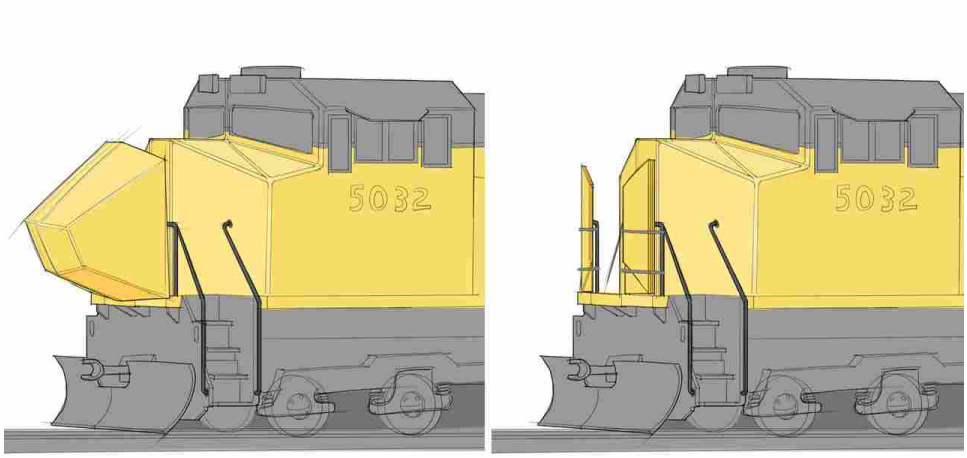

Figure 6.1: Initial concept for an origami-inspired deployable fairing based on rigid folding panels. Left: The fairing in its deployed state. Right: the fairing in its stowed (folded) state.

allow coupling of locomotives without restricting the walkway between locomotives for when the locomotive is not in the lead position.

The fairing design presented here is based on thick origami. When thickness is introduced in an origami-based mechanism, that thickness must be accommodated to prevent self intersection of panels. Many techniques have been introduced which accommodate thickness in origami-based mechanisms. These techniques include changing the shape of the panel to prevent intersection [6, 9], moving the hinges of the pattern out of plane to prevent interference [23], replacing revolute joints with flexible hinges that allow out of plane movement [31, 43], and modifying the crease pattern to create space for stacking panels [32].

The foldable fairing presented here is also based on non-developable origami. A developable surface is one where the Gaussian curvature is zero i.e. it can be flattened into a plane without stretching the material. Because traditional origami starts with a flat sheet of paper and is folded into a 3D shape, it can likewise be unfolded back into a flat sheet and is therefore developable. In terms of origami, we define a developable pattern to be one that does not require cutting and gluing to achieve its final shape. Although cutting and gluing is typically eschewed in origami, in engineering design some interesting and useful designs have come about by cutting and gluing paper to create non-developable patterns such as egg-box patterns [57], tube patterns [59],

and three-dimensional polyhedra-based patterns [60]. Thickness-accommodation techniques have been applied primarily to developable patterns. This work explores the potential of thickness-accommodation techniques being applied to patterns that are non-developable. We will discuss the additional considerations that must be made when dealing with non-developable thick origami and the constraints that some techniques have with non-developable vertices.

This document outlines the approach taken and the results achieved to design a foldable locomotive fairing based on non-developable thick origami that can meet the general requirements of both the deployed and stowed states. Additional constraints and functional requirements that the design must achieve are discussed. A final fairing design that has been shown to meet all the space constraints and functionality requirements and decreases aerodynamic drag by over 16 percent is discussed and prototypes shown.

6.2 Background

The block-like shape of modern freight locomotives makes for poor aerodynamics when compared to the shape of high-speed passenger trains [73]. The design of today's locomotives has been driven largely by operational constraints and cost to manufacture rather than its aerodynamic performance. The resulting locomotive shape is unfortunate because it results in high aerodynamic drag and contributes to higher fuel consumption at cruising speed.

The attachment of a nose fairing to a locomotive could reduce the total drag on a train. However, for such an attachment to work with current locomotives, it must not interfere with the functionality of the front locomotive coupling action. Locomotives are often coupled at the front and rear of a long train. A locomotive with a large static nose-fairing attached would need the fairing to be taken on and off every time it were coupled and uncoupled with other locomotives.

Modern freight locomotives have many features at the front that could potentially interfere with a fairing. Some of these features include the windshields, headlights, front door, stairs, walk-way, coupler, snow plow, hand rails, and electrical and pneumatic connectors. The implementation of a fairing on the front of a locomotive must take these functions into consideration. The foldable fairing presented here seeks to overcome the challenges inherent with a static fairing by providing stowed and deployed configurations that can meet the requirements of both the lead and non-lead locomotive positions.

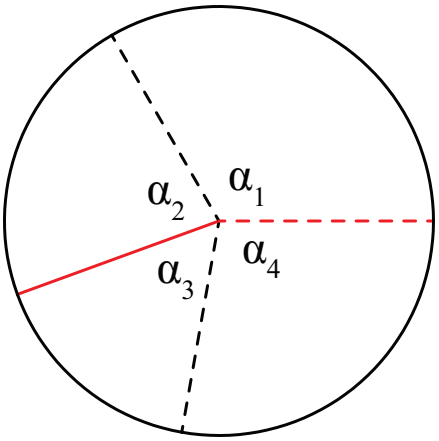

Figure 6.2: A degree-4 vertex.

6.2.1 Thick Origami

An origami pattern can be seen as a system of spherical linkages where panels are links and fold lines are hinges [3]. A subset of origami patterns are called rigidly-foldable patterns. Rigidly-foldable origami patterns do not require the bending of facets while folding and only require deflection of the creases to fold. When modeled as a linkage these patterns will have a positive mobility. This is important in thick origami applications because thick panels are often too stiff to provide deflection similar to what can occur in traditional origami. Using rigid foldable patterns in thick origami ensures that strain energy is not stored in panels and the mechanism will be easier to actuate.

The degree-4 vertex, such as the one shown in Figure 6.2, is the building block of many origami patterns. The angles between fold lines are called sector angles and are represented by α_1 through α_4. For a degree-4 vertex to fold flat it must satisfy the Kawasaki-Justin theorem [61] which states that for flat-foldable vertices:

$$\alpha_1 - \alpha_2 + \alpha_3 - \alpha_4 = 0. \tag{6.1}$$

When paper is creased, its stiffness is reduced along the crease line allowing the paper to act as both the links and hinges in a mechanism [74]. When designing thick origami mechanisms, the crease lines of an origami pattern are replaced by a surrogate hinge [44]. These hinges can

be revolute joints, compliant members, or rolling contact based joints [75]. For the locomotive fairing, the load carrying capacity of the hinges is an important consideration. The wind load that a fairing experiences during operation translates into large forces so traditional pin-joint hinges are used in the fairing design.

Thickness-accommodation techniques considered for use in the foldable fairing include the axis-shift technique [23] and the offset-panel technique [9]. These techniques are chosen due to the fact that flat panels are used in their construction, special hinges or an extra number of hinges are not required, and revolute joints can be used.

The offset-panel technique accommodates thickness through the use of panels that are offset from the zero-thickness origami pattern but maintain the same hinge locations as the zero-thickness origami pattern. An example degree-4 offset panel vertex is illustrated in Figure 6.3. We can see from this figure that the hinge lines intersect at a point, maintaining the same spherical linkage as the original origami pattern. The offset panel technique has been utilized in various thick origami applications [10], however the application of the technique to non-developable patterns is a new area of exploration. An advantage of using the offset panel technique for non-developable patterns is that the same techniques and methods used for developable patterns can be applied. This is because the technique does not modify the spherical linkage of the zero-thickness pattern.

The axis-shift technique shifts the hinge lines rather than the panels of a zero-thickness pattern to accommodate thickness. An example degree-4 axis-shift vertex is illustrated in Figure 6.4. As seen in this figure, because the hinge lines have been shifted, they no longer lie in the same plane when folded flat and they no longer intersect at a point throughout the folding motion. Because of this the linkage is no longer a spherical mechanism but is a spatial 4-R mechanism. This mechanism is know as the Bennett Linkage where opposing link pairs are equal in length and have the same rotational axis twist. The criteria for the mechanism to achieve mobility given in [23] are:

$$\alpha_1 + \alpha_3 = \alpha_2 + \alpha_4 = \pi \tag{6.2}$$

$$d_1 = d_3, d_2 = d_4 \tag{6.3}$$

$$\frac{d_1}{d_2} = \frac{\sin(\alpha_1)}{\sin(\alpha_2)} \tag{6.4}$$

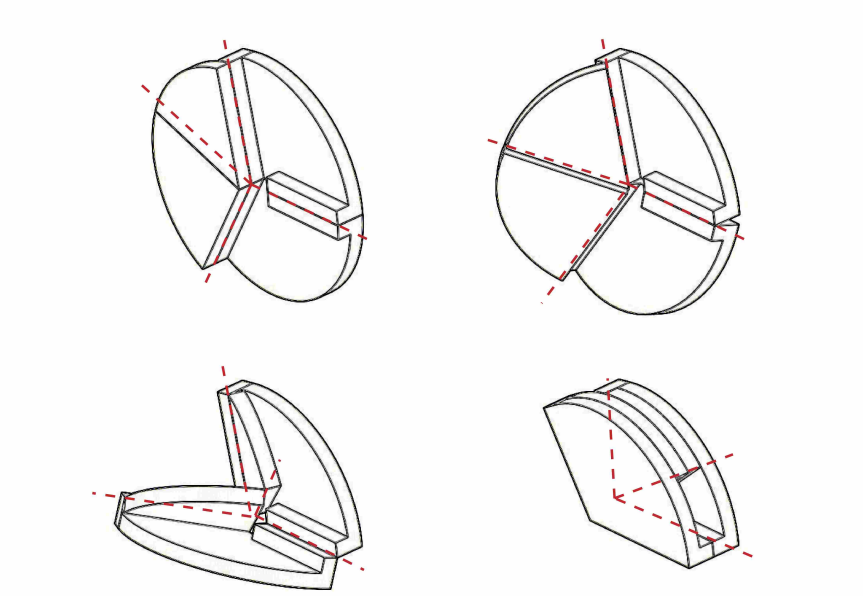

Figure 6.3: An example offset-panel vertex. Hinges are indicated by red dashed lines.

The first criteria listed in Equation 6.2 corresponds with the flat foldability criteria given in Equation 6.1. This means patterns modified with the axis-shift technique must be flat foldable to achieve mobility. Another consequence of Equation 6.2 is that the sum of all the sector angles α_1 through α_4 must equal 2π. This means that the axis-shift technique for degree-4 vertices as discussed in [23] is only applicable to developable origami patterns. The foldable locomotive fairing design presented here, however, is based on a non-developable origami pattern and therefore axis-shift technique cannot be utilized in its design. Due to this constraint, the offset-panel technique was utilized to accommodate thickness for the foldable fairing mechanism.

6.3 Approach

The first step in designing a foldable fairing was to determine the space in which a deployed and stowed fairing could occupy on the front of a locomotive. For a deployed fairing it was determined that the space as shown in Figure 6.5 could be occupied without interfering with the view of the engineer, the headlights, plow, or other frontal features. For the stowed position it was determined that the fairing could occupy the space as shown in Figure 6.6 without interfering with the walkway between locomotives or any of the coupling mechanisms between locomotives. In

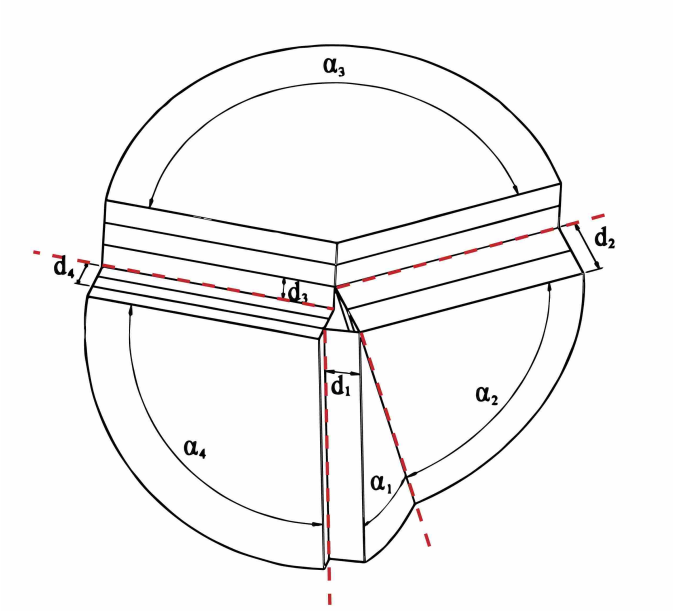

Figure 6.4: An example axis-shift vertex. Hinges are indicated by red dashed lines.

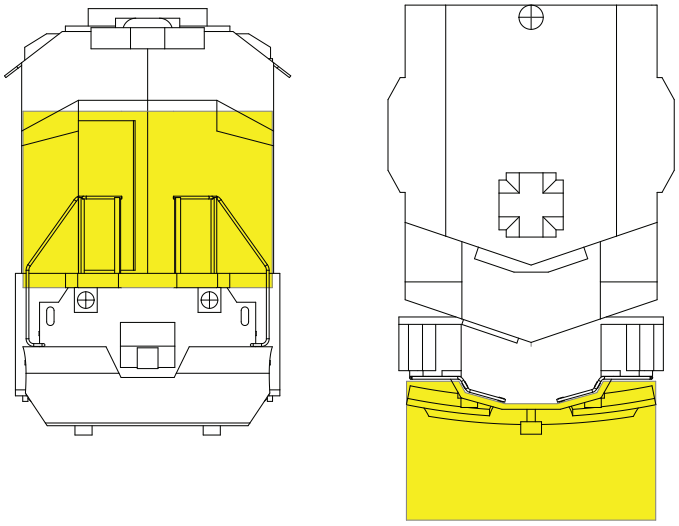

Figure 6.5: Design volume for the deployed fairing. Usable area is highlighted in yellow.

addition to the spatial requirements of the fairing, operational considerations such as the difficulty and time required to deploy and stow the fairing had to be taken into account. The reliability and maintenance requirements were also considered.

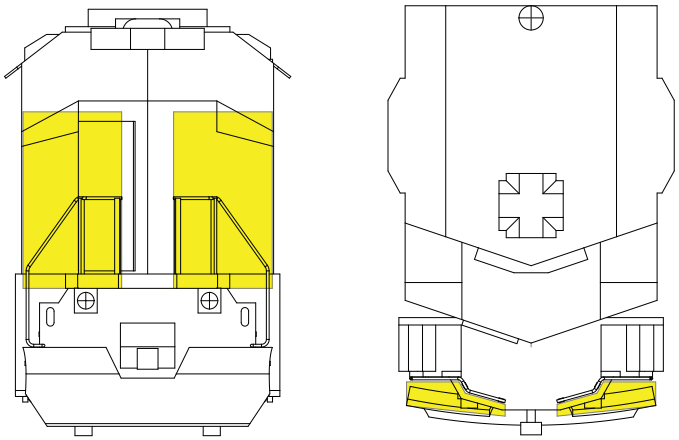

Figure 6.6: Design volume for the fairing in the stowed configuration. Usable area is highlighted in yellow.

The approach taken to design the fairing involved iteration in the following process: Concept Generation, Concept Evaluation, Concept Selection, Design Optimization, and Design Validation.

6.4 Concept Generation

With the functional requirements of the fairing in mind, concepts for reconfigurable designs were generated. Many concept fairings, such as those illustrated in Figures 6.1 and 6.7, were generated including inflatable concepts, tension fabric concepts, and folding rigid panel concepts. Although origami was the initial source of inspiration for the foldable fairing project, concepts were not limited to origami-related ideas. Many possible methods of deployment were considered as long as the concept could achieve the desired deployed and stowed shapes. Over 40 different concepts were generated by project participants.

6.5 Concept Evaluation

All of the concepts generated could achieve the desired deployed and stowed shapes so the large number of initial concepts was narrowed down by evaluating them for robustness, cost, ease of use, and maintenance requirements. By evaluating the various concepts against the requirements, the number of concepts was narrowed to two: a rigid panel fairing and a tension fabric fairing. Inflatable fairings were ruled out due to maintenance concerns and the time involved in

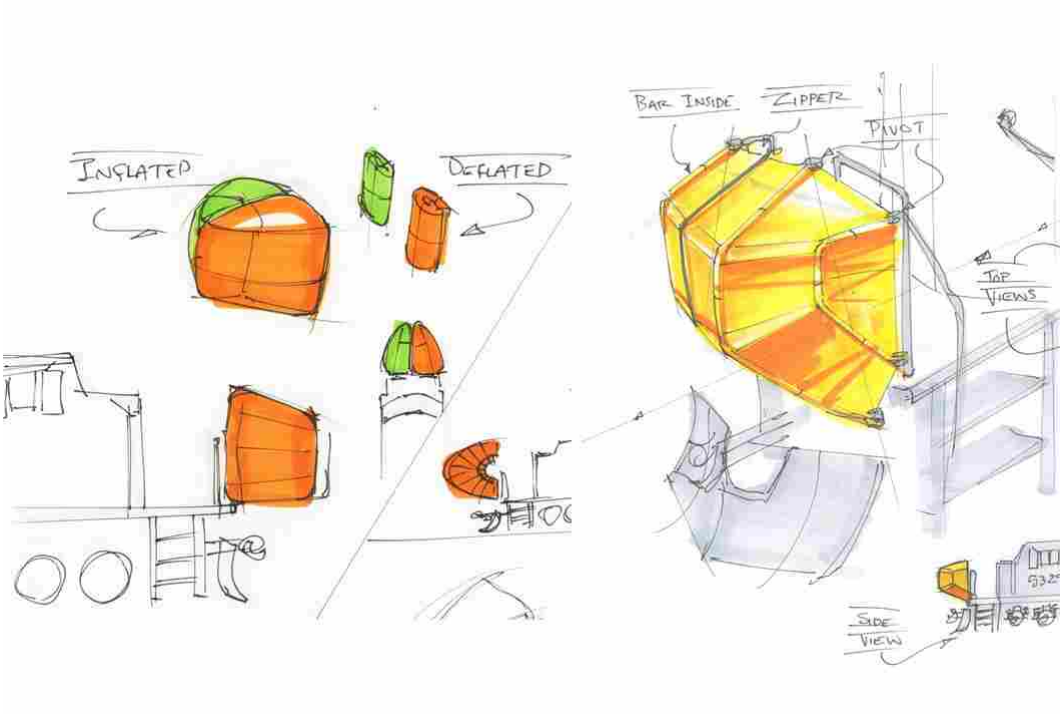

Figure 6.7: Fabric-based design concepts. Left: inflatable fairing concept sketch. Right: tension-fabric-based fairing concept.

inflating and deflating. The other concepts could be considered subsets of these two main types of fairings. To select between the two main categories, the concepts were explored in more depth with prototypes.

6.5.1 Flat-panel-based concept

A flat panel based concept was created that utilized two foldable halves. This concept, as shown in Figure 6.8, folds into two flat panel stacks with a space between the panel stacks that would leave the deck-to-deck walkway between locomotives open.

The pattern of the flat-panel-based concept was designed to approximate the shape of a bullet with flat panels. Because a bullet is a non-developable shape, the origami pattern created to approximate it was also non-developable. This is uncharacteristic of origami as origami is usually folded from paper which is a developable surface.

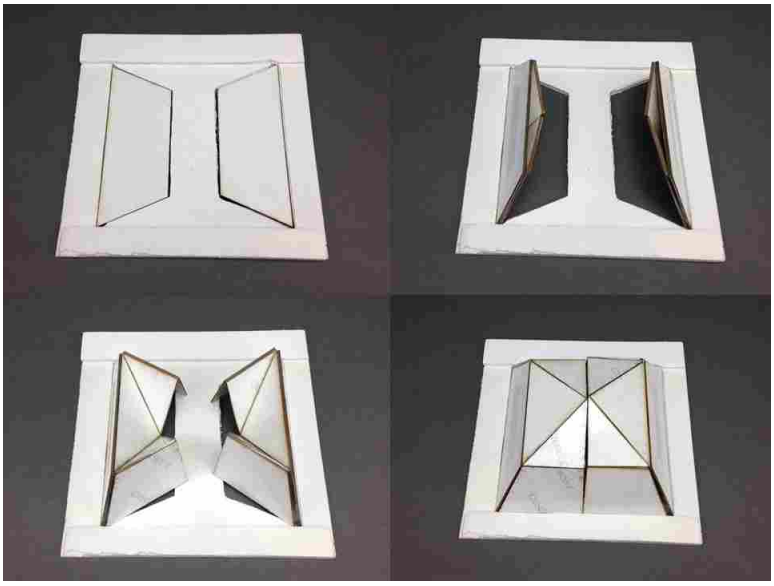

Figure 6.8: Proof-of-concept prototype of the non-developable origami-based flat panel design.

Each half of the rigid-panel-based folding fairing is comprised of degree-4 vertices. The prototype shown in Figure 6.8 utilizes two degree-4 vertices in each half. For each half of the fairing to be able to fold flat, every vertex must be flat foldable.

6.5.2 Fabric-based concept

The fabric-based concept is based on a fabric membrane stretched across a folding frame. The concept is inspired by many collapsible fabric-based structures such as tents and awnings. The requirements of a nose fairing however are very different from that of many fabric based deployables. Tents and awnings usually deform easily in strong winds. A fabric-based fairing however would need to maintain its shape in strong headwinds to provide consistent aerodynamic performance.

A fabric-based design is shown in Figure 6.9. The design utilizes two folding frame members for each half and an architectural fabric that is stretched across the frame. The fabric and folding frame members are attached to a rigid frame. The two halves are secured by means of a zipper that joins the fabric.

Figure 6.9: Scaled prototype of tension-fabric concept.

6.6 Concept Selection

After evaluating both the rigid-panel and tension-fabric designs, the rigid-panel-based fairing was chosen for further development for a number of reasons. First the rigid-panel fairing was evaluated to be more robust against colliding objects. Second the ability of a rigid-panel fairing to maintain its shape under heavy wind loads was much greater than a fabric-based fairing. Third, a simpler geometry simplified the optimization process to reduce drag.

6.7 Design Optimization

To determine an optimal geometry for a nose fairing within the design volume, an optimization study was conducted [76]. In this study fairing geometries were evaluated using computational fluid dynamic (CFD) software STAR-CCM+, based on the K-epsilon turbulence model at a steady state 80 KPH fluid flow. Over 140 different nose fairings were evaluated and a multidimensional polynomial regression was used to determine optimal geometries.

This study was conducted in two parts. The first study evaluated a parametric nose fairing design where fairing length (α), tip width (β), and tip height (δ) as illustrated in Figure 6.10, were varied within a constraint space. The resulting optimal design of is shown in Figure 6.11.

The resulting geometry of was significantly different than the starting geometry. The front face of the optimal design had a slope of 70 degrees, much steeper than anticipated. It is hypothesised that this steep angle helps to direct flow up onto the top of the locomotive rather than

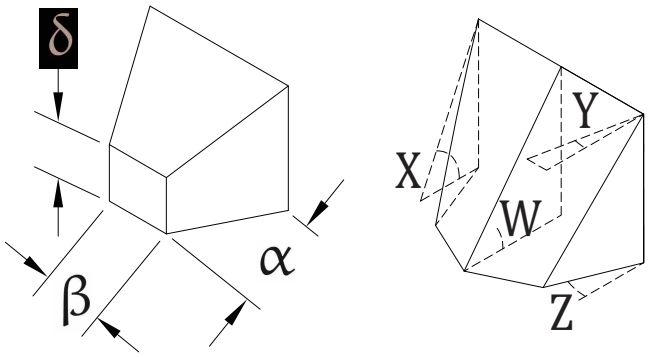

Figure 6.10: Parameters used in the first study (left) and the second study (right).

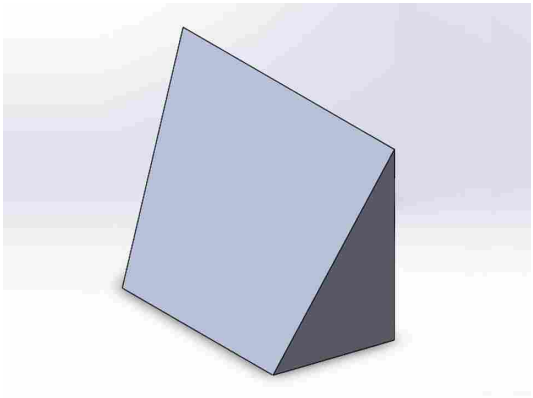

Figure 6.11: Optimized shape of the first CFD study.

stagnating on the blunt windshields. This fairing geometry reduced drag on the locomotive by approximately 15 percent.

The second study took the optimized shape of the first study as the starting point and then varied four angles: the inside top angle, outside top angle, top-plane side angle, and the bottom-plane side angle. The resulting optimal design is shown in Figure 6.12. This design reduced drag on the locomotive by approximately 17 percent.

The geometry of this second study is similar to the first firing in size and they have similar trailing edge angles, but the front face is concave rather than flat. Concave counter-intuitive geometry supports the conclusion that directing more flow onto the top of the locomotive helps reduce drag more than directing flow to the sides. When examining the sides and top of the locomotive, the sides tend to have more features that would create drag (e.g. hand-rail supports, vents, wheel assemblies). The fluid flow around around a locomotive is highly complex and a counter-intuitive

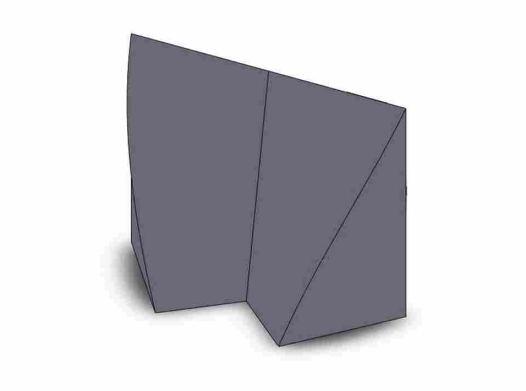

Figure 6.12: Optimized shape of the second CFD study.

fairing shape can reduce flow separation and consequently overall drag. Following these studies, wind tunnel tests were also performed to validate the CFD models. The results of the wind tunnel tests showed the same drag reduction trends as the CFD model and overall drag reduction values were the same.

Because the shape of the second study is a curved surface and the goal was to have a flat-panel fairing, the curved shape would have to be approximated with flat panels. Based on the hypothesis that channeling fluid flow over the top of the locomotive is what helped achieve higher performance, flat panel designs which would do the same where explored. A design which proved to have similar performance as the curved design is shown in Figure 6.13. This design was created by taking the geometry of the first study and adding vanes to each side to help channel the flow onto the top of the locomotive. CFD analysis showed that this flat-panel design reduced drag by over 16%. Although not as high as the 17% drag reduction for the curved shape, the trade-off in stowability and manufacturability was deemed acceptable and the simplified geometry with vanes was chosen for the final design.

6.8 Final Fairing Design

The fairing shape shown in Figure 6.13 was selected and the folding pattern to fold the non-developable shape into the allotted space (see Figure 6.6) was designed. The folding pattern for one half of the final fairing design is shown in Figure 6.14. Because it is a non-developable surface, it cannot be folded in a single piece of paper. It starts out as two pieces which are then

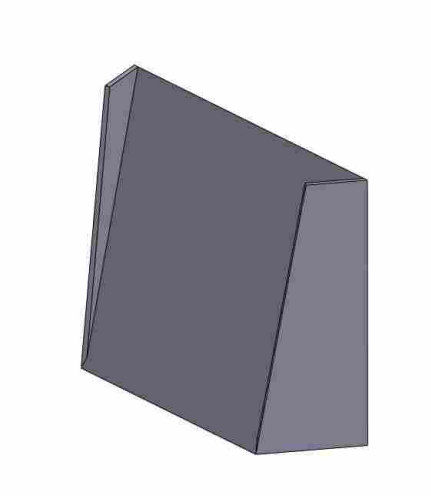

Figure 6.13: Simplified shape that gives performance similar to the curved shape of the second study.

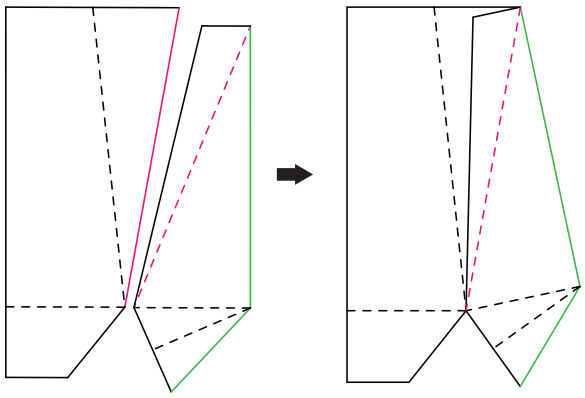

Figure 6.14: Fold pattern of the non-developable fairing design. Red lines indicate where the face panel attaches to the side panel. Green lines indicate where the panels attach to the frame.

attached together along the diagonal of the other piece to form the vane. The green lines in Figure 6.14 are attached to a static frame which is attached to the locomotive. The frame and the three panels which attach to it form a degree-4 origami vertex, or a spherical mechanism. The other panels of the fairing form an open loop non-spherical spatial linkage once the fold axes are shifted to accommodate for thickness.

An eighth-scale prototype of the final design, as shown in Figure 6.15, was constructed as a proof of concept of the folding motion and thickness-accommodation methods. 0.85 mm sheet metal was used as the panel material and steel piano hinges were used at the fold lines. The prototype was assembled using spot welds. Offsets in the panels were created by spot welding

Figure 6.15: Eighth-scale prototype constructed from sheet metal.

additional strips of sheet metal between the panels and hinges so that the correct offset distance was achieved. Magnets were used in this eighth-scale prototype to secure the panels in either the deployed or stowed positions, where latches would be used in the full-scale design.

The eighth-scale prototype shares many of the same design aspects as the full scale design but there are some differences such as the panel material choice. Although solid steel panels worked well for the eighth scale prototype, for the full scale prototype this would be prohibitively heavy, a concern not for the locomotive's sake but for the operator who must manually deploy and stow the fairing. A high-strength steel and high density polyethylene foam (HDPE) sandwich panel, shown in Figure 6.16 was selected as the material for the production version of the fairing. This material keeps the weight of the fairing within an acceptable range for one person operation without compromising stiffness or strength. The material is also economical when compared to aluminum sandwich panel options.

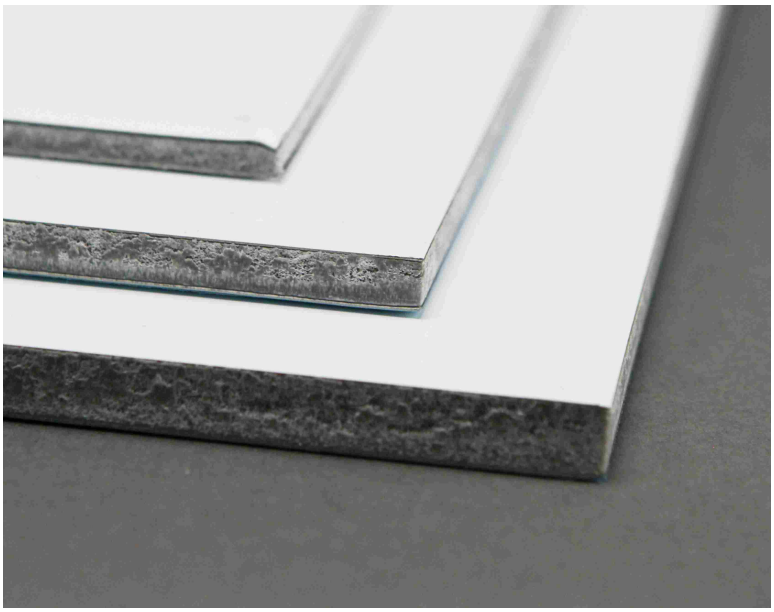

Figure 6.16: Composite high-strength steel and HDPE foam sandwich panel selected as the panel material for the full scale fairing design.

6.9 Design Validation through Full-Scale Prototype

To validate the operational aspects of the folding fairing, a full-scale prototype was constructed. The prototype, as shown in Figure 6.17, was constructed with plywood and piano hinges. Latching hardware was used to secure the fairing in the open and closed positions. The prototype was installed on an operational locomotive. Figure 6.18 provides a perspective of the size compared to a 158 cm tall person. When deployed the fairing is 2.35 meters wide, 1.9 meters tall from the top of the train deck, and is 1.7 meters off the ground. The functionality of the foldable fairing design was validated by demonstrating it could be deployed and stowed by one person in under 30 seconds. The fairing also did not interfere with the features or functionality of the locomotive.

6.10 Conclusion

The design of an origami-inspired deployable locomotive fairing has been presented. The fairing design is based on non-developable thick origami. Considerations for the design of non-developable thick origami mechanisms has also been discussed and we have shown that the offset-panel technique has advantages when it comes to accommodating thickness in non-developable patterns. The geometry of the fairing was optimized using CFD analysis and multi-dimensional

Figure 6.17: Full-scale prototype on a freight locomotive shown in both the stowed configuration (right) and deployed configuration (right). Photo has been modified to remove locomotive identity.

polynomial regression. The resulting fairing design is estimated to reduce drag by over 16% for a locomotive cruising at 80 kph. The design was verified with wind tunnel testing. The deploy-stow functions were demonstrated on a full-scale prototype attached to a freight locomotive. The fairing can be easily deployed and stowed by one person in under 30 seconds and does not interfere with any of the features or functionality of the locomotive. Using statistics of freight hauling trains, it is estimated that the addition of the nose fairing onto a fleet of locomotives can save over $2,000,000 a year in fuel costs per fleet of 1000 trains.

Figure 6.18: The top of the fairing stands 3.6 meters tall from the ground. An 158 cm tall person provides a visual indication of the fairing size. Photo has been modified to remove locomotive identity.

CHAPTER 7. CONCLUSION

7.1 Conclusions

Thickness-accommodation techniques enable designers to create novel and useful mechanisms in origami-inspired engineered systems. Because every technique has its capabilities and limitations, the selection of which thickness-accommodation technique to utilize depends on the application. The detailed review of existing techniques here provides a valuable tool for those unfamiliar with thickness-accommodation in origami-inspired design. Hybrid techniques which have been introduced here, enable new capabilities that are unique for each technique combination. Hybrid techniques will allow designers to create origami-inspired engineered systems that overcome many of the challenges of existing approaches and have unprecedented performance.

The split-vertex technique that has been presented offers the advantage of accommodating thickness without introducing holes or protrusions in the mechanism while maintaining single-degree-of-freedom kinematics. The technique shows promise in applications where a sealed surface must be maintained such as in collapsible containers or shelters. The flat construction of split-vertex mechanisms lend themselves well to planar fabrication techniques.

The application of thickness-accommodation techniques to non-developable origami patterns has been introduced here. The considerations that must be made when dealing with non-developable patterns in thick-origami are discussed. For some thickness-accommodation techniques the transition from developable to non-developable patterns is minor but for other techniques such as the axis-shift technique, there are major changes that must occur.

The design of an origami-inspired deployable locomotive fairing has been presented. The fairing design is based on non-developable thick origami. The resulting fairing design is estimated to reduce drag by over 16% for a locomotive cruising at 80 kph. The deploy-stow functions of this fairing were demonstrated on a full-scale prototype attached to a freight locomotive. The fairing can be easily deployed and stowed by one person in under 30 seconds, does not interfere with the

features or functionality of the locomotive, and can save millions of dollars a year in fuel costs for rail lines.

7.2 Future Work

I propose the following areas of potential future research that would provide value to the field of origami-inspired engineering projects.

- Further develop the theory and applications of non-developable thick origami.
- Further develop thickness-accommodation techniques which are based on compliance in the folding mechanism and do not require rigid-foldable patterns.
- Utilize the principles of thickness-accommodation for novel and useful applications.

REFERENCES

[1] Kuribayashi, K., Tsuchiya, K., You, Z., Tomus, D., Umemoto, M., Ito, T., and Sasaki, M., 2006. "Self-deployable origami stent grafts as a biomedical application of ni-rich tini shape memory alloy foil." *Materials Science and Engineering: A,* **419**(1), pp. 131–137. 1, 31

[2] Zirbel, S. A., Lang, R. J., Thomson, M. W., Sigel, D. A., Walkemeyer, P. E., Trease, B. P., Magleby, S. P., and Howell, L. L., 2013. "Accommodating thickness in origami-based deployable arrays." *Journal of Mechanical Design,* **135**(11), p. 111005. 1, 18, 20, 32

[3] Bowen, L. A., Grames, C. L., Magleby, S. P., Howell, L. L., and Lang, R. J., 2013. "A classification of action origami as systems of spherical mechanisms." *Journal of Mechanical Design,* **135**(11), p. 111008. 1, 32, 51, 66

[4] Lang, R. J., Tolman, K. A., Crampton, E. B., Magleby, S. P., and Howell, L. L., 2016. "A review of thickness-accommodation techniques in origami-inspired engineering." *Applied Mechanics Reviews,* **Accepted Manuscript**(TBD). 1, 4, 23, 31, 32

[5] Tolman, K. A., Lang, R. J., Magleby, S. P., and Howell, L. L., 2017. "Split-vertex technique for thickness-accommodation in origami-based mechanisms." In *Proceedings of the ASME 2017 International Design Engineering Technical Conferences & Computers and Information in Engineering Conference* Paper #IDETC2017-68018. 2, 31, 60

[6] Tachi, T., 2011. "Rigid-foldable thick origami." In *Origami*^{5}. CRC Press, pp. 253–264. 4, 6, 9, 31, 43, 64

[7] Lang, R. J., Nelson, T. G., Magleby, S. P., and Howell, L. L., 2016. "Thick rigidly foldable origami mechanisms based on synchronized offset rolling contact elements." In *Proceedings of the ASME 2016 International Design Engineering Technical Conferences & Computers and Information in Engineering Conference* Paper #IDETC2016-59747. 4, 15, 17, 18, 23, 24, 32

[8] Edmondson, B. J., Lang, R. J., Magleby, S. P., and Howell, L. L., 2014. "An offset panel technique for thick rigidly foldable origami." In *Proceedings of the ASME 2014 International Design Engineering Technical Conferences & Computers and Information in Engineering Conference* Paper #DETC2014-35606. 7

[9] Edmondson, B. J., Lang, R. J., Morgan, M. R., Magleby, S. P., and Howell, L. L., 2016. "Thick rigidly foldable structures realized by an offset panel technique." In *Origami*^{6}, K. Miura, T. Kawasaki, T. Tachi, R. Uehara, R. J. Lang, and P. Wang-Iverson, eds. American Mathematical Society, pp. 149–161. 7, 32, 64, 67

[10] Morgan, M. R., Lang, R. J., Magleby, S. P., and Howell, L. L., 2016. "Towards developing product applications of thick origami using the offset panel technique." *Mechanical Sciences,* **7**(1), p. 69. 8, 67

[11] Lewis, T. S., 1858. Folding-bench, Dec. 21 US Patent 22,371. 9

[12] Nellis, G., 1866. Improved folding table, Oct. 2 US Patent 58,462. 9

[13] Sulzbacheb, M., 1869. Improved folding mattress, July 6 US Patent 92,396. 9

[14] Hoberman, C., 1988. Reversibly expandable three-dimensional structure United States Patent No. 4,780,344. 9

[15] Hoberman, C., 2010. Folding structures made of thick hinged sheets, Sept. 14 US Patent 7,794,019. 9, 26, 32

[16] Yoshimura, Y., 1951. "On the mechanism of a circular cylindrical shell under axial compression." *NACA Technical Reports*(NACA-TM-1390). 10, 26

[17] Gattas, J. M., Wu, W., and You, Z., 2013. "Miura-base rigid origami: Parameterizations of first-level derivative and piecewise geometries." *Journal of Mechanical Design,* **135**(11), p. 111011. 10

[18] Lee, T.-U., and Gattas, J. M., 2016. "Geometric design and construction of structurally stabilized accordion shelters." *Journal of Mechanisms and Robotics,* **8**(3), p. 031009. 10

[19] Trautz, M., and Künstler, A., 2009. "Deployable folded plate structures - folding patterns based on 4-fold-mechanism using stiff plates." In *Proceedings of IASS Symposium 2009, Valencia*, pp. 2306–2317. 10, 18, 32

[20] Trautz, M., and Buffart, H., 2013. "Construction approach for deployable folded plate structures without transversal joint displacement." In *Proceedings of the First Conference Transformables*. 10

[21] De Temmerman, N., Mollaert, M., Van Mele, T., Beaumesnil, B., and De Laet, L., 2006. "Development of a foldable mobile shelter system." In *Adaptables 2006, Proceedings of the International Conference on Adaptability in Design and Construction*, Vol. 2, pp. 13–17. 10

[22] De Temmerman, N., Mollaert, M., Van Mele, T., and De Laet, L., 2007. "Design and analysis of a foldable mobile shelter system." *International Journal of Space Structures,* **22**(3), pp. 161–168. 10, 28, 31

[23] Chen, Y., Peng, R., and You, Z., 2015. "Origami of thick panels." *Science,* **349**(6246), pp. 396–400. 12, 13, 32, 55, 56, 64, 67, 68

[24] You, Z., and Chen, Y., 2012. *Motion Structures: Deployable Structural Assemblies of Mechanisms*. Spon Press, New York. 12

[25] Bennett, G., 1903. "A new mechanism." *Engineering,* **76**(12), pp. 777–778. 12

[26] Beggs, J. S., 1966. *Advanced mechanism*. Macmillan. 13

[27] Myard, F., 1931. "Contribution à la géométrie des systèmes articulés." *Bulletin de la Société Mathématique de France,* **59**, pp. 183–210. 13

[28] Bricard, R., 1927. *Leçons de cinématique*., Vol. II: Cinématique Appliquée Gauthier-Villars, Paris. 13

[29] Chen, Y., Feng, H., Ma, J., Peng, R., and You, Z., 2016. "Symmetric waterbomb origami." *Proc. R. Soc. A,* **472**(2190), p. 20150846. 13

[30] Hoberman, C., 1991. Reversibly expandable structure United States Patent No. 4,981,732. 14

[31] Zirbel, S. A., Wilson, M. E., Magleby, S. P., and Howell, L. L., 2013. "An origami-inspired self-deployable array." In *ASME 2013 Conference on Smart Materials, Adaptive Structures and Intelligent Systems*, American Society of Mechanical Engineers, pp. SMASIS2013–3296. 14, 20, 64

[32] Ku, J. S., and Demaine, E. D., 2016. "Folding flat crease patterns with thick materials." *Journal of Mechanisms and Robotics,* **8**(3), p. 031003. 14, 32, 35, 37, 64

[33] Ku, J. S., and Demaine, E. D., 2016. "Rigid folding analysis of offset crease thick folding." In *Proceedings of the IASS Annual Symposium 2016 "Spatial Structures in the 21st Century"*, K. Kawaguchi, M. Ohsaki, and T. Takeuchi, eds. 15, 32

[34] Scientific American, 1889. "Jacob's ladder." *Scientific American,* **61**, October 12, p. 227. 16

[35] Wikipedia, 2016. Jacob's ladder (toy) — wikipedia, the free encyclopedia [Online; accessed 26-August-2016]. 16

[36] Hillberry, B. M., and Hall Jr, A. S., 1976. Rolling contact prosthetic knee joint, Mar. 23 US Patent 3,945,053. 16

[37] Halverson, P. A., Bowden, A. E., and Howell, L. L., 2012. "A compliant mechanism approach to achieving specific quality of motion in a lumbar total disc replacement." *International Journal of Spine Surgery,* **6**(1), pp. 78–86. 16

[38] Collins, C. L., 2003. "Kinematics of robot fingers with circular rolling contact joints." *Journal of Robotic Systems,* **20**(6), pp. 285–296. 16

[39] Cannon, J. R., and Howell, L. L., 2005. "A compliant contact-aided revolute joint." *Mechanism and Machine Theory,* **40**(11), pp. 1273–1293. 17

[40] Halverson, P. A., Howell, L. L., and Magleby, S. P., 2010. "Tension-based multi-stable compliant rolling-contact elements." *Mechanism and Machine Theory,* **45**(2), pp. 147–156. 17

[41] Cai, J., 2016. "Kinematic analysis of foldable plate structures with rolling joints." *Journal of Mechanisms and Robotics,* **8**(3), p. 034502. 17

[42] Peraza-Hernandez, E. A., Hartl, D. J., and Lagoudas, D. C., 2016. "Kinematics of origami structures with smooth folds." *Journal of Mechanisms and Robotics,* **8**(6), p. 061019. 19

[43] Pehrson, N. A., Magleby, S. P., Lang, R. J., and Howell, L. L., 2016. "Introduction of monolithic origami with thick-sheet materials." In *Proceedings of the IASS Annual Symposium 2016 "Spatial Structures in the 21st Century"*, K. Kawaguchi, M. Ohsaki, and T. Takeuchi, eds. 20, 21, 32, 64

[44] Delimont, I. L., Magleby, S. P., and Howell, L. L., 2015. "A family of dual-segment compliant joints suitable for use as surrogate folds." *Journal of Mechanical Design,* **137**(9), p. 092302. 21, 66

[45] Durney, M. W., 2002. Method for precision bending of a sheet of material and slit sheet therefor, Nov. 19 US Patent 6,481,259. 21

[46] Howell, L. L., 2001. *Compliant Mechanisms*. John Wiley & Sons, Inc. 21

[47] Howell, L. L., Magleby, S. P., and Olsen, B. M., eds., 2013. *Handbook of Compliant Mechanisms*. John Wiley & Sons, Ltd. 21

[48] Delimont, I. L., Magleby, S. P., and Howell, L. L., 2015. "Evaluating compliant hinge geometries for origami-inspired mechanisms." *Journal of Mechanisms and Robotics,* **7**(1), p. 011009. 21

[49] Sessions, J., Pehrson, N., Tolman, K., Erickson, J., Fullwood, D., and Howell, L. L., 2016. "A material selection and design method for multi-constraint compliant mechanisms." In *Proceedings of the ASME 2016 International Design Engineering Technical Conferences & Computers and Information in Engineering Conference*. 22

[50] Peraza-Hernandez, E. A., Hartl, D. J., Malak Jr, R. J., and Lagoudas, D. C., 2014. "Origami-inspired active structures: a synthesis and review." *Smart Materials and Structures,* **23**(9), p. 094001. 31

[51] Thrall, A., and Quaglia, C., 2014. "Accordion shelters: a historical review of origami-like deployable shelters developed by the us military." *Engineering Structures,* **59**, pp. 686–692. 31

[52] Silverberg, J. L., Evans, A. A., McLeod, L., Hayward, R. C., Hull, T., Santangelo, C. D., and Cohen, I., 2014. "Using origami design principles to fold reprogrammable mechanical metamaterials." *Science,* **345**(6197), pp. 647–650. 31

[53] Zhou, X., Wang, H., and You, Z., 2014. "Mechanical properties of miura-based folded cores under quasi-static loads." *Thin-Walled Structures,* **82**, pp. 296–310. 31

[54] Randall, C. L., Gultepe, E., and Gracias, D. H., 2012. "Self-folding devices and materials for biomedical applications." *Trends in Biotechnology,* **30**(3), pp. 138–146. 31

[55] Miura, K., and Natori, M., 1985. "2-D array experiment on board a space flyer unit." *Space Solar Power Review,* **5**, pp. 345–356. 31, 63

[56] Wilson, L., Pellegrino, S., and Danner, R., 2013. "Origami sunshield concepts for space telescopes." In *54th AIAA/ASME/ASCE/AHS/ASC Structures, Structural Dynamics, and Materials Conference*. 31

[57] Xie, R., Chen, Y., and Gattas, J. M., 2015. "Parametrisation and application of cube and eggbox-type folded geometries." *International Journal of Space Structures,* **30**(2), pp. 99–110. 33, 51, 54, 64

[58] Filipov, E. T., Tachi, T., and Paulino, G. H., 2015. "Origami tubes assembled into stiff, yet reconfigurable structures and metamaterials." *Proceedings of the National Academy of Sciences,* **112**(40), pp. 12321–12326. 33, 51, 54

[59] Filipov, E. T., Paulino, G. H., and Tachi, T., 2016. "Origami tubes with reconfigurable polygonal cross-sections." *Proc. R. Soc. A,* **472**(2185), p. 20150607. 33, 51, 64

[60] Overvelde, J. T., Weaver, J. C., Hoberman, C., and Bertoldi, K., 2017. "Rational design of reconfigurable prismatic architected materials." *Nature,* **541**(7637), pp. 347–352. 33, 51, 65

[61] Demaine, E. D., and ORourke, J., 2007. *Geometric folding algorithms*. Cambridge university press Cambridge. 33, 52, 66

[62] Huffman, D. A., 1976. "Curvature and creases: A primer on paper." *IEEE Trans. Computers,* **25**(10), pp. 1010–1019. 34

[63] Lang, R. J., Magleby, S., and Howell, L. L., 2016. "Single degree-of-freedom rigidly foldable cut origami flashers." *Journal of Mechanisms and Robotics,* **8**(3), p. 031005. 34, 39, 60

[64] Miura, K., 1970. "Proposition of pseudo-cylindrical concave polyhedral shells." In *Proceedings of IASS Symposium on Folded Plates and Prismatic Structures*. 37

[65] Tachi, T., 2010. "Geometric considerations for the design of rigid origami structures." In *Proceedings of the International Association for Shell and Spatial Structures (IASS) Symposium*, Vol. 12, pp. 458–460. 37

[66] Tachi, T., 2009. "Generalization of rigid foldable quadrilateral mesh origami." In *Symposium of the International Association for Shell and Spatial Structures (50th. 2009. Valencia). Evolution and Trends in Design, Analysis and Construction of Shell and Spatial Structures: Proceedings*, Editorial Universitat Politècnica de València. 37

[67] Evans, T. A., Lang, R. J., Magleby, S. P., and Howell, L. L., 2015. "Rigidly foldable origami gadgets and tessellations." *Royal Society open science,* **2**(9), p. 150067. 37

[68] Evans, T. A., Lang, R. J., Magleby, S. P., and Howell, L. L., 2015. "Rigidly foldable origami twists." *Origami,* **6**, pp. 119–130. 44

[69] Bern, M., Demaine, E. D., Eppstein, D., Kuo, E., Mantler, A., and Snoeyink, J., 2003. "Ununfoldable polyhedra with convex faces." *Computational Geometry,* **24**(2), pp. 51–62. 52

[70] Yellowhorse, A., Tolman, K. A., Magleby, S. P., and Howell, L. L., 2017. "Optimization of origami-based tubes for lightweight deployable structures." In *Proceedings of the ASME 2017 International Design Engineering Technical Conferences & Computers and Information in Engineering Conference* Paper #IDETC2017-67274. 57, 58

[71] Chai, W., and Chen, Y., 2010. "The line-symmetric octahedral bricard linkage and its structural closure." *Mechanism and Machine Theory,* **45**(5), pp. 772 – 779. 58

[72] You, Z., and Kuribayashi, K., 2009. "Expandable tubes with negative poisson's ratio and their applications in medicine." In *Origami*^{4}, R. J. Lang, ed. A K Peters, pp. 117–128. 63

[73] Lukaszewicz, P., 2007. "Running resistance-results and analysis of full-scale tests with passenger and freight trains in sweden." *Proceedings of the Institution of Mechanical Engineers, Part F: Journal of Rail and Rapid Transit,* **221**(2), pp. 183–193. 65

[74] Francis, K., Blanch, J., Magleby, S., and Howell, L., 2013. "Origami-like creases in sheet materials for compliant mechanism design." *Mechanical Sciences,* **4**(2), pp. 371–380. 66

[75] Lang, R. J., Nelson, T., Magleby, S., and Howell, L., 2017. "Thick rigidly foldable origami mechanisms based on synchronized offset rolling contact elements." *Journal of Mechanisms and Robotics,* **9**(2), p. 021013. 67

[76] Stucki, C., and Maynes, D., 2016. "Aerodynamic design of a locomotive fairing." In *APS Division of Fluid Dynamics Meeting Abstracts*. 73